Journal of Structural Geology 97 (2017) 1–22

Contents lists available at ScienceDirect

Journal of Structural Geology

journal homepage: www.elsevier.com/locate/jsg

Interacting faults

D.C.P. Peacock [a, *], C.W. Nixon [a], A. Rotevatn [a], D.J. Sanderson [b], L.F. Zuluaga [a]

[a] Department of Earth Science, University of Bergen, Allégaten 41, 5007, Bergen, Norway
[b] Engineering and the Environment, University of Southampton, Highfield, Southampton, SO17 1BJ, UK

ARTICLE INFO

Article history:
Received 14 August 2016
Received in revised form
8 February 2017
Accepted 18 February 2017
Available online 21 February 2017

Keywords:
Faults
Interaction
Geometry
Kinematics
Strain
Chronology

ABSTRACT

The way that faults interact with each other controls fault geometries, displacements and strains. Faults rarely occur individually but as sets or networks, with the arrangement of these faults producing a variety of different fault interactions. Fault interactions are characterised in terms of the following: **1) Geometry** – the spatial arrangement of the faults. Interacting faults may or may not be *geometrically linked* (i.e. physically connected), when fault planes share an intersection line. **2) Kinematics** – the displacement distributions of the interacting faults and whether the displacement directions are parallel, perpendicular or oblique to the intersection line. Interacting faults may or may not be *kinematically linked*, where the displacements, stresses and strains of one fault influences those of the other. **3) Displacement and strain in the interaction zone** – whether the faults have the same or opposite displacement directions, and if extension or contraction dominates in the acute bisector between the faults. **4) Chronology** – the relative ages of the faults. This characterisation scheme is used to suggest a classification for interacting faults. Different types of interaction are illustrated using metre-scale faults from the Mesozoic rocks of Somerset and examples from the literature.

© 2017 Elsevier Ltd. All rights reserved.

1. Introduction

Faults commonly develop as a network, within which the constituent faults can display a range of lengths, sizes, and orientations. A number of different interactions can occur within a network as the faults form geometric and kinematic relationships with each other (e.g., Fossen et al., 2005; Frankowicz and McClay, 2010; Nixon et al., 2014a; Duffy et al., 2015).

What, however, is the best way to interpret interacting faults and how does one differentiate between different types of fault interaction? To address these questions, we investigate the geometry, kinematics and age relationships of different fault interactions. We produce a scheme for identifying, interpreting, describing and ultimately classifying the ways in which any two faults may interact.

There has been considerable interest in the interaction and linkage of stepping, sub-parallel, synchronously active faults, especially normal (e.g., Larsen, 1988; Morley et al., 1990; Peacock and Sanderson, 1991; Leeder and Jackson, 1993; Walsh et al., 1999) and strike-slip faults (e.g., Wilcox et al., 1973; Rodgers, 1980; Biddle and Christie-Blick, 1985; Woodcock and Fischer, 1986; Aydin and Schultz, 1990). Peacock and Sanderson (1991), for example, show stages in the interaction and linkage of stepping normal faults (Fig. 1). There has been much less interest, however, in the interaction and linkage of non-parallel faults, which may or may not be synchronous (e.g., Fig. 2).

A fault network can form within a single stress field, producing interactions between coeval faults (Fig. 3a), including linkage of sub-parallel faults (e.g., Peacock and Sanderson, 1991; Cartwright et al., 1995; Gawthorpe et al., 2003; Fossen et al., 2005; Bull et al., 2006; Nixon et al., 2014a; Fossen and Rotevatn, 2016). A fault network can also form by the mutual abutting and cross-cutting relationships of conjugate faults (e.g., Odonne and Massonnat, 1992; Nicol et al., 1995; Kelly et al., 1998; Ferrill et al., 2009; Nixon et al., 2011). In contrast, some fault networks form by the overprinting or superposition of two or more stress fields, producing interactions between faults of different ages or type (Fig. 3b), resulting in abutting and cross-cutting relationships between the non-coeval fault sets (e.g., Fossen et al., 2005; Maerten et al., 2001; Bailey et al., 2005; Nixon et al., 2014a). Some fault networks form also by the reactivation of pre-existing faults (e.g., Maerten et al., 2001; Giba et al., 2012; Nixon et al., 2014a; Duffy et al., 2015). Such interacting faults may be:

* Corresponding author.
E-mail address: hermangedge@gmail.com (D.C.P. Peacock).

http://dx.doi.org/10.1016/j.jsg.2017.02.008
0191-8141/© 2017 Elsevier Ltd. All rights reserved.

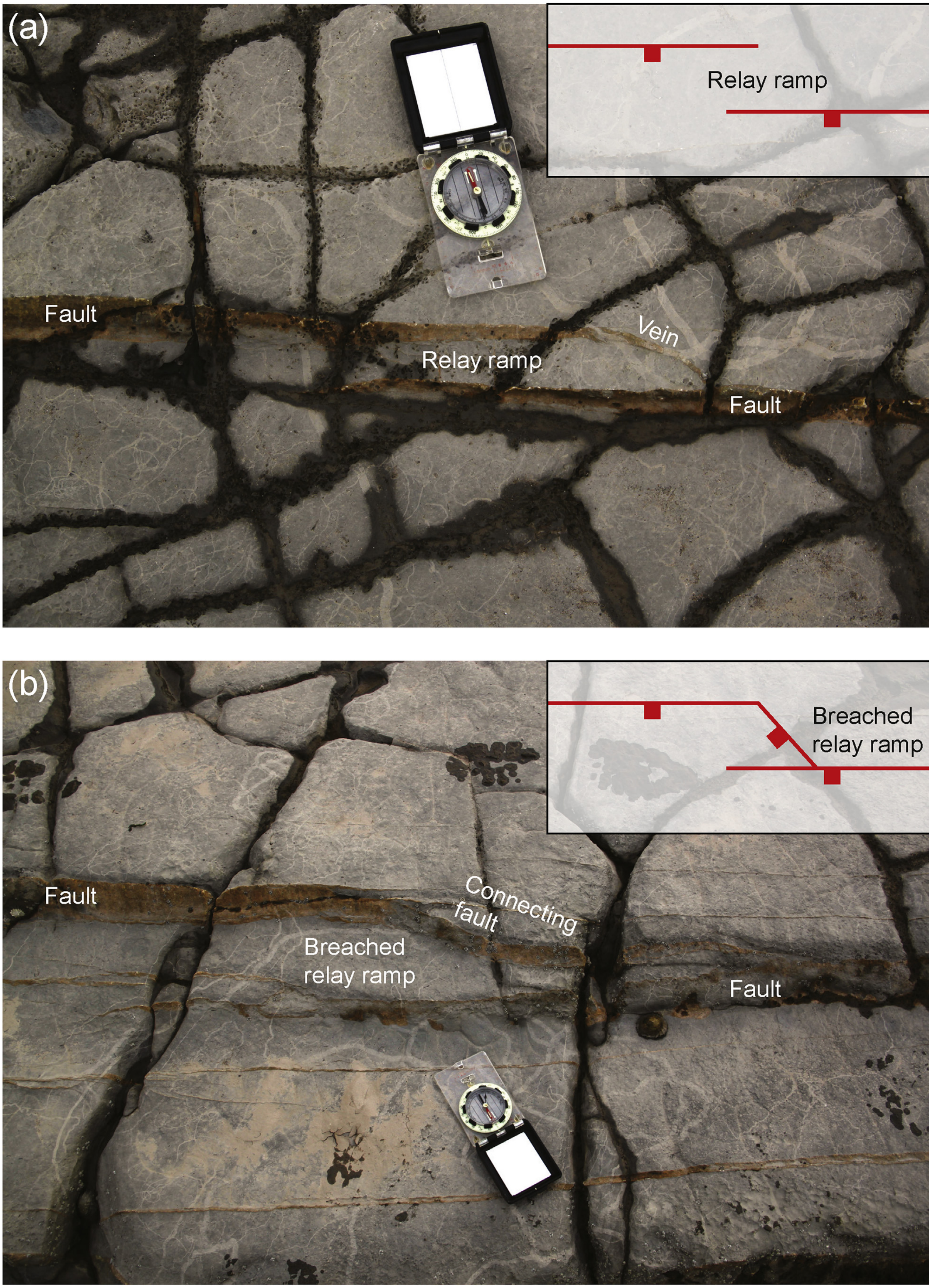

Fig. 1. Examples of interaction and linkage of sub-parallel, synchronous normal faults that step in map view across a relay ramp on Liassic limestone bedding planes, Somerset, UK. (a) The two faults step, with bedding rotated across a relay ramp. Veins cut across the relay ramp, these being precursors to breaching of the relay ramp. (b) The relay ramp is breached by a connecting fault.

- *Geometrically linked* (where two faults are connected at an intersection line; approximately synonymous with *geometrical coherence* of Walsh and Watterson, 1991),
- *Kinematically linked* (where the displacements or strains of two or more faults are related, e.g., Nixon et al., 2014b; Peacock et al., 2016; approximately synonymous with *kinematic coherence* of Walsh and Watterson, 1991), or
- Both geometrically- and kinematically-linked.

Fault interaction produces areas of local stress concentration and perturbation that affect the geometry and kinematics of the faults (e.g., Kattenhorn et al., 2000; Maerten, 2000; Bourne and Willemse, 2001; Maerten et al., 2002). These stress concentrations can cause the formation of secondary structures within damage zones, where structures are focussed and commonly have different orientations than in the surrounding areas (e.g., Kim et al., 2004; Fossen et al., 2005; Bastesen and Rotevatn, 2012; Choi et al., 2016). Understanding the characteristics of these fault interactions is important as they can provide useful information about the deformation history. Fault interactions can also influence fluid flow by providing pathways or acting as barriers (e.g., Knipe, 1992; Manzocchi et al., 1999; Aydin, 2000; Rotevatn et al., 2009a). They are of economic significance because they can provide localised zones of mineralisation (e.g., Curewitz and Karson, 1997) and cause major uncertainty in the prediction of reservoir behaviour (e.g., Fossen et al., 2005; Gartrell et al., 2006; Jolley et al., 2010).

In spite of their importance, no thorough characterisation of fault interactions appears to have been published. Thus, we aim to characterise and classify interacting faults and to present a clear and precise terminology for describing the different fault interactions. We focus on describing field examples from Somerset, UK, where a history of different tectonic regimes provides a rich array of fault interactions. Examples from the literature are also used (Table 1). This provides a framework for establishing a workflow for analysing interacting faults based on determining their geometric and kinematic relationships and their chronology. We have recently published a glossary of terms related to fault and other fracture networks (Peacock et al., 2016) and use that terminology here.

2. Geological background of field examples

To illustrate the range of fault interactions that occur, we use photographs of faulted upper Triassic and lower Jurassic Liassic limestones and shales from the Somerset coast between Lilstock and Blue Anchor, UK (Fig. 4). These examples are used because of the high quality of the exposures, they are photogenic, the tectonic history is well constrained, and the area is freely accessible (except around high tide, when care is needed). Structures in the Triassic marls and Liassic limestones and shales in Somerset, demonstrate Mesozoic basin development and Tertiary (Alpine) basin inversion (e.g., Dart et al., 1995). Several palaeostress orientation analyses of the Bristol Channel Basin have been published (e.g., Peacock and Sanderson, 1992; Dart et al., 1995; Nemčok et al., 1995; Glen et al., 2005). The deformation history is as follows:

1. Normal faults striking ~095° and related gentle folds were caused by ~ N-S extension during Mesozoic development of the Bristol Channel Basin (e.g., Nemčok et al., 1995). The normal faults have displacements of up to hundreds of metres (Whittaker and Green, 1983). The Liassic limestones and shales in Somerset are unlikely to have been buried more than ~2 km depth, based on the thicknesses of the overlying sequence in the region.
2. Evidence for sinistral shear followed by dextral reactivation of some 095° striking normal faults includes the steepening of beds in relay ramps and shear along vein systems around some normal faults (Peacock and Sanderson, 1999). This suggests σ_1 was oriented ~ NW-SE. Hibsch et al. (1995) describe Upper Jurassic to Early Cretaceous E-W to WNW-ESE transtension elsewhere in England, while Vandycke and Bergerat (2001) describe strike-slip faulting, with σ_1 orientated NNE-SSW to N-S in the Cretaceous Chalk of the Isle of Wight.
3. The Tertiary deformation that produced the Alpine Mountain Belt further south and southeast in Europe is commonly marked in southern England by the reverse-reactivation of Mesozoic and older structures (e.g., Underhill and Patterson, 1998). Evidence for N-S contraction includes N-S striking calcite veins, E-W striking thrusts, E-W striking folds (including crenulation cleavage), and reverse-reactivation of some of the larger displacement 095° striking normal faults (Kelly et al., 1999; Peacock and Sanderson, 1999).
4. The reverse-reactivated normal faults are cut by strike-slip faults conjugate about ~010° and with displacements of up hundreds of metres (e.g., Whittaker, 1972; Dart et al., 1995).
5. Joints post-date faulting and may represent the reduction of Alpine stresses (Rawnsley et al., 1998). The post-faulting age of the joints is indicated by their curving and abutting relationships with the faults (Peacock, 2001). Vandycke (2002) also describes joints that record Neogene NE-SW extension across SE England.

The initiation and development of these faults are described by Willemse et al. (1997) and Peacock and Sanderson (1999).

The description of the range of different fault interactions in Sections 3–8 is an attempt to generalise fault interactions, applicable to all fault classes (normal, reverse, strike-slip and oblique-slip) at all scales. This scheme will be of use for describing fault patterns, especially in understanding related deformation patterns, as occurs in fault networks. These different types of fault interaction are illustrated using meso-scale examples from exposures in the Mesozoic sedimentary rocks of Somerset, UK. To show that the range of fault interactions is not unique to the scales, lithologies and tectonic setting of the Somerset exposures, we also present examples from elsewhere in Table 1.

3. Geometric relationships between interacting faults

We characterise the geometric relationships between the faults based on whether or not, and how, they *intersect* (Fig. 5). The following relationships can exist between any two faults:

- The faults are isolated from each other, do not interact and are not connected. The faults exposed in Somerset (and generally throughout the World) are characterised by their segmentation, interaction and linkage, with faults that are truly isolated in 3D being very rare. For example, the fault zone in Somerset described by Peacock and Sanderson (1991) is composed of a series of interacting and linked segments, although the zone itself appears to be approximately isolated in map view.
- The faults interact as they *approach* each other, but they need not be connected by smaller faults or other fractures, i.e., they are *kinematically* linked but not *geometrically* linked. Fig. 5(a) shows conjugate strike-slip faults that appear to approach each other but not actually meet. Interaction is indicated by a set of solution seams in the acute bisector between the faults.
- One fault *abuts* another fault. The faults may have originally been unconnected or one may have splayed off the other, and they may have formed in the same deformation event or be from

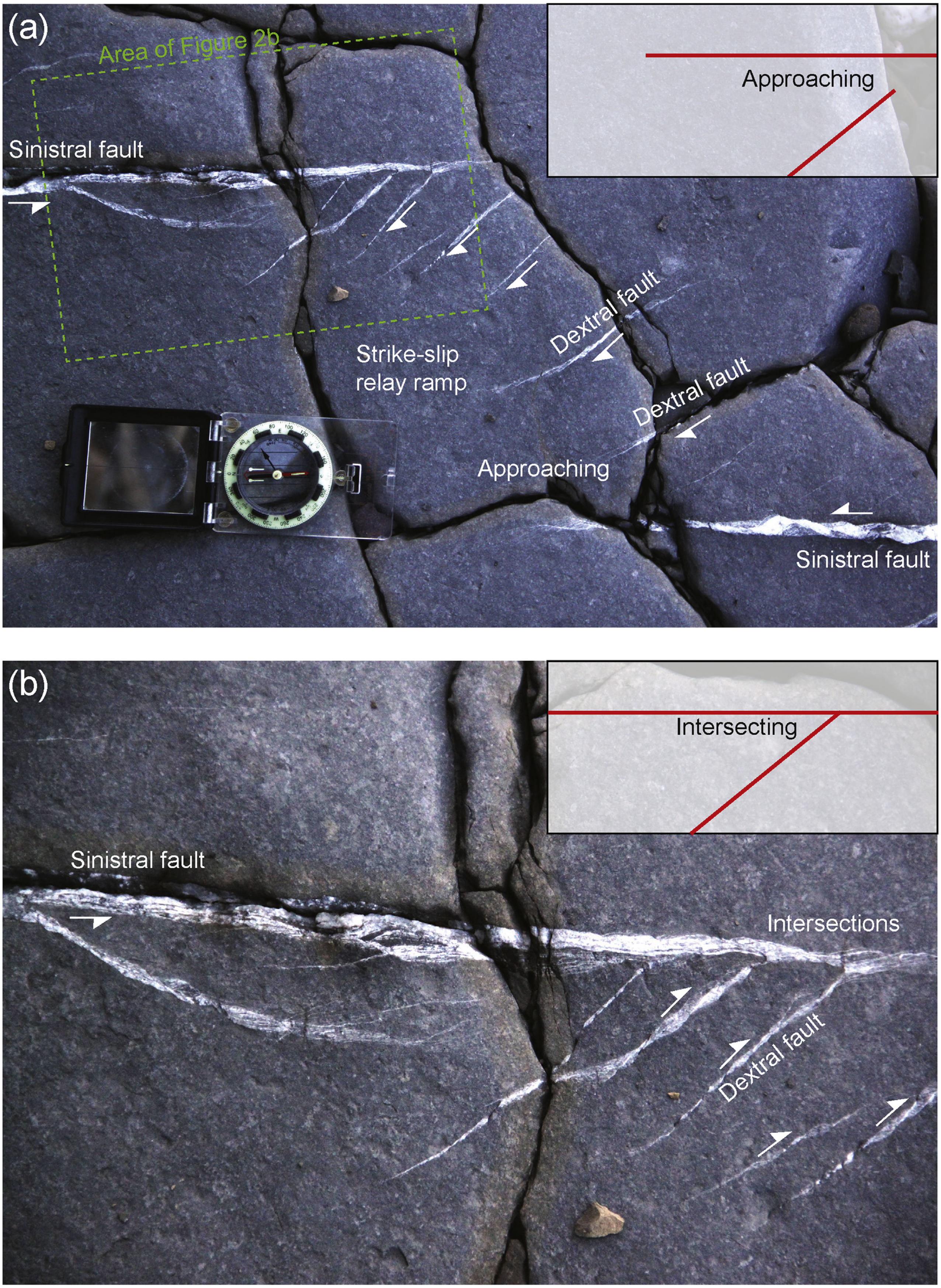

Fig. 2. Example of interaction and intersection between non-parallel strike-slip faults in a strike-slip relay ramp (Peacock and Sanderson, 1995) on a Liassic limestone bedding plane, East Quantoxhead, Somerset. The senses of displacements are determined from pull-apart geometries (e.g., Willemse et al., 1997). (a) Two sub-parallel sinistral faults step, with strain accommodated in the strike-slip relay ramp by a series of dextral faults. Four of the dextral faults approach, but do not intersect, the sinistral faults. (b) Close-up of part of the structure shown in Fig. 2(a), showing some of the dextral faults that intersect a sinistral fault.

different episodes. Fig. 5(b) shows two normal faults at an angle of about 30° to each other, with the one fault abutting the other. Care is needed, however, with interpreting the development of such geometries, because similar geometries can be created by faults that splay and faults that approach and intersect (Fig. 6). Fig. 5(b) also shows earlier faults cut by the abutting faults.
- An earlier fault is cut by and displaced by a later fault. Fig. 5(c) shows a normal fault zone cut and displaced by a dextral strike-slip fault.
- Two faults mutually crosscut each other. Fig. 5(d) shows two strike-slip fault zones that appear to mutually crosscut each other in the way shown by Horsfield (1980) and by Ferrill et al. (2009).

Fig. 7 shows an additional characterisation for intersections between normal faults, based on the relative dip directions of the faults and whether the intersecting fault is in the hanging-wall or footwall of the fault that it intersects. Examples of these different geometries from Somerset are shown in Fig. 8. There may be some practical difficulties in using this classification, however, for example if the intersecting faults show a Y pattern where neither fault trace is straight, such as would occur at a triple junction. Such a classification, however, may be of use and is expandable to other fault systems, i.e., reverse, strike-slip and oblique-slip faults.

4. Kinematic relationships between interacting faults

We define the kinematic relationships between faults based on the relationships between the intersection line (the line along which faults meet) and the displacement direction (Fig. 9). Please note that the examples shown (e.g., Fig. 9) have intersection *points* that represent the intersection *lines* on the planes of view. The following end-member relationships exist:

- The intersection line is parallel to the displacement direction. Fig. 9(a) shows two normal faults that are linked across a relay ramp by a breaching fault (e.g., Peacock and Sanderson, 1991). The breaching fault connects with the two stepping faults along steeply dipping intersection lines that are sub-parallel to the displacement directions of the faults. Such displacement that is parallel to the intersection line is kinematically simple as it avoids significant wall rock deformation (e.g., Walsh et al., 1999).
- The intersection line is perpendicular to the displacement direction. Fig. 9(b) shows a bend along a dextral fault zone represented by two intersections that has created a fault-bound lens and a pop-up. The intersection lines are approximately perpendicular to the fault displacement direction. Displacement perpendicular to the intersection is kinematically more complicated than where the displacement is parallel to the intersection because it would involve significant volumetric strain and wall rock deformation (e.g., Walsh et al., 1999). This behaviour is illustrated by the pop-up shown in Fig. 9(b).
- The intersection line is parallel to the displacement direction of one fault and perpendicular to the displacement direction of the other fault. Fig. 9(c) shows normal faults that are displaced by strike-slip faults such that the fault intersection lines are sub-parallel to the displacement directions on the normal faults and approximately perpendicular to the displacement directions on the strike-slip faults.

Note, however, that intersection lines may be curved (e.g., Butler, 1982, figure 7a).

5. Displacement and strains between the interacting faults

We characterise fault interactions based on the relative shear senses of the interacting faults (Fig. 10). The following criteria are used:

- Antithetic relationship, where the faults have opposite senses of displacement, and this is approximately perpendicular to the intersection line. Fig. 10(a) shows antithetic normal faults, which have opposite senses of displacement to each other and with each having displacement approximately perpendicular to the intersection line. Displacement on these faults will cause space problems near the interaction zone, with displacement variations along the faults having to be taken up by strain in the wall rocks (e.g., Ferrill et al., 2009).
- Synthetic relationship, where the faults have the same senses of displacement, approximately perpendicular to the intersection line. Fig. 10(b) shows synthetic normal faults, which have the same senses of displacement to each other and with each having displacement approximately perpendicular to the intersection line.
- *Neutral* relationship, where the faults have the same senses of displacement, and that is approximately parallel to the intersection line (cf. Walsh et al., 1999). We use the term "neutral" because there is no tendency for either extension or contraction in the acute bisector, with little or no space problem caused by interaction between the faults. Fig. 10(c) shows intersecting normal faults with a neutral relationship, i.e., the faults have the same senses of displacement as each other, with displacement approximately parallel to the intersection line.

Fault interactions can also be characterised by the dominant strains in the acute bisectors between the faults (Fig. 11):

- Interacting faults will tend to be synthetic when extension dominates in the acute bisector Fig. 11(a) shows drag along a sinistral fault accommodated by rotation of shale laminae involving small dextral faults. Extension dominates in the acute bisector between the intersecting faults, with voids filled by calcite cement. Note that contraction may dominate in the obtuse bisector of such a fault pattern.
- Interacting faults will tend to be antithetic when contraction dominates in the acute bisector. Fig. 11(b) shows synchronously active conjugate strike-slip faults, with contraction dominating in the acute bisector. Note that extension may dominate in the obtuse bisector of such a geometric relationship, and some extension even occurs in the acute bisector of the example shown in Fig. 11(b), as indicated by calcite along the fault planes.

6. Relative age relationships between interacting faults

Fig. 12 shows examples of intersecting faults with different age relationships in the Liassic limestones and shales of Somerset. Fig. 12(a) two intersecting normal faults that appear to have been synchronously active, and belong to the same deformation event. The folding of bedding between the two faults indicates synchronous activity. Fig. 12(b) shows a normal fault cut by a later dextral strike-slip fault. *Trailing* is where two new faults or other fracture types are connected via an older fault or other fracture, on which renewed displacement occurs to connect the two later faults or fractures (Peacock et al., 2016). Whilst field examples of trailing fault geometries have not been observed in the Mesozoic rocks in Somerset, Fig. 12(c) shows calcite veins that show a trailing relationship. Fig. 12(d) shows the East Quantoxhead fault, which has ~

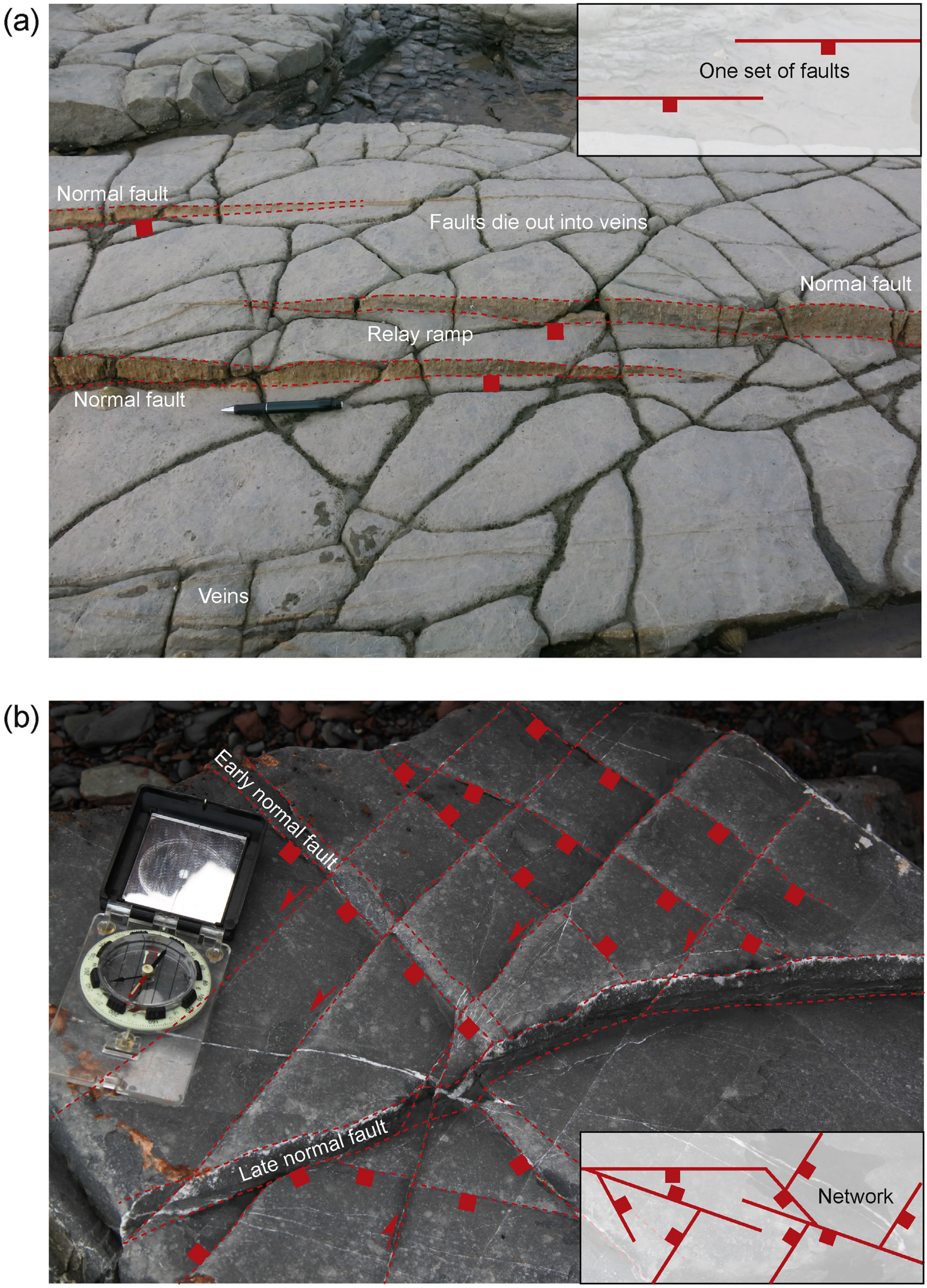

Fig. 3. Different types of fault network and interactions. (a) Normal faults on a bedding plane of Liassic limestone, East Quantoxhead, Somerset. A single stress field, producing interactions between coeval faults, including linkage of sub-parallel faults (e.g., Peacock and Sanderson, 1991). (b) Network of faults on a limestone bedding plane, Watchet, Somerset. The fault network was formed by the overprinting and superposition of two or more stress fields, producing interactions between faults of different ages, resulting in abutting and crosscutting relationships between the non-coeval fault sets (e.g., Duffy et al., 2015). Note that the block was not *in situ*.

Table 1
Examples of the different types of fault interactions described in this paper. In this context, “small” means exposure-scale examples of the type illustrated from Somerset, while “large” means examples tens of metres across or larger, e.g., observable on seismic data.

Relationship	Figure in this manuscript	Other small examples	Large examples
Approaching faults	Figs. 5a, 14	Crider and Peacock (2004, figure 6a), Morley (2014, figures 12 and 13)	Tapponnier and Molnar (1977, figure 2), Taylor and Peltzer (2006, figure 1)
Abutting faults	Fig. 5b	Peacock (1991, figure 8)	Lonergan et al. (1998, figure 9), Nixon et al. (2014a, figure 10)
Cutting faults	Fig. 5c	Kelly et al. (1999, figure 3)	Proffett (1977, figure 4), Needham et al. (1996, figures 10 and 11)
Abutting normal fault in hanging-wall, synthetic	Fig. 8a	Michie et al. (2014, figure 5b)	Figure 11a, Hesthammer et al. (2001, figure 2), Needham et al. (1996, figure 9)
Abutting normal fault in hanging-wall, antithetic	Fig. 8b	Peacock and Zhang (1994, figure 4)	Figure 11b, Nixon et al. (2014a, figure 11)
Abutting normal fault in footwall, synthetic	Fig. 8c	Michie et al. (2014, figure 5b)	Figure 11c, Tesfaye et al. (2008, figure 7a)
Abutting normal fault in footwall, antithetic	Fig. 8d	Michie et al. (2014, figure 5b)	Figure 11d, Chorowicz (2005, figure 17), Putz-Perrier and Sanderson (2010, figure 10)
Mutually cutting faults	Fig. 9d	Nicol et al. (2013, figure 1c)	Nicol et al. (1995, figure 5)
Branch line parallel to displacement	Fig. 9a	Kim et al. (2003, figure 13)	Woodcock and Rickards (2003, figure 3)
Branch line normal to displacement	Fig. 9b	Kelly et al. (1998, figure 6)	Taylor and Peltzer (2006, figure 12)
Different displacement directions	Fig. 9c	Kelly et al. (1998, figure 12)	Guest et al. (2006, figure 4)
Antithetic faults	Fig. 10a	Peacock and Sanderson (1994, figure 11), Mollema and Antonellini (1999, figure 12), Bourne and Willemse (2001, figure 7)	Tesfaye et al., (2008, figure 16), Giba et al. (2012, figure 3), Moore et al. (2013, figure 3)
Synthetic faults	Fig. 10b	Peacock (1991, figure 7), Kelly et al. (1998, figure 11)	Paton and Underhill (2004, figure 3), ten Veen et al. (2009, figure 1), Carne and Little (2012, figure 1)
Neutral intersection	Fig. 10c	Peacock (2002, figure 1b)	Griffiths (1980, figure 3)
Extensional Y	Fig. 11a	Willemse et al. (1997, figure 7), Kim et al. (2003, figure 9b)	Molnar and Tapponnier (1975, figure 4), Nur et al. (1989, figure 10), Platt and Becker (2013, figure 1)
Contractional Y	Fig. 11b	Kim et al. (2003, figure 9a), Katz et al. (2004, figure 3)	Chorowicz (2005, figure 12a)
Synchronous faults	Fig. 12a	Kelly et al. (1998, figure 6), Tewksbury et al. (2014, figure 2)	Ding et al. (2013, figure 8)
Different age faults	Fig. 12b	Kelly et al. (1998, figure 12)	Pizzi and Garaldini (2009, figure 2), Nixon et al. (2014a, figure 16)
Trailing faults	Fig. 12c		Nixon et al. (2014a, figure 15)
Fault reactivation	Fig. 12d	Ehteshami-Moinabadi (2014, figure 6)	Underhill and Patterson (1998, figure 9)

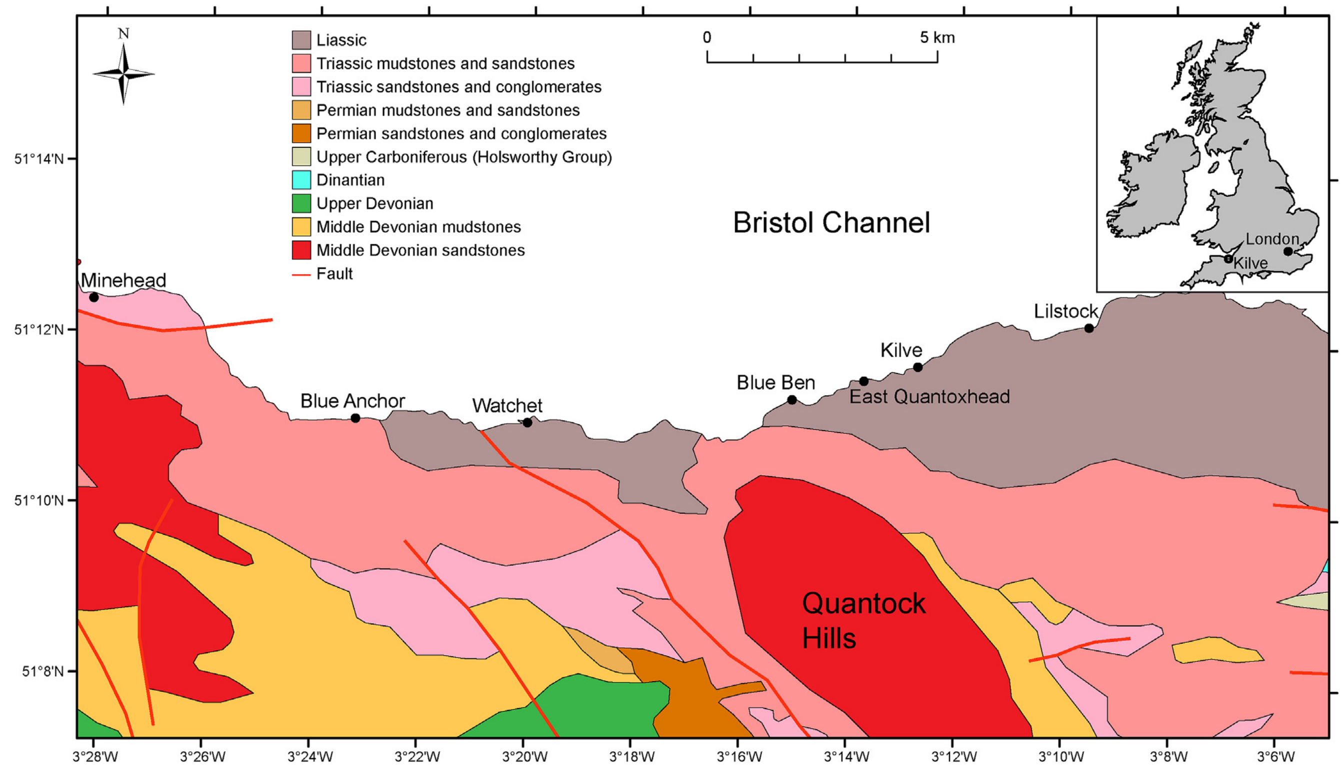

Fig. 4. Geological map of part of the Somerset coast, reproduced with the permission of the British Geological Survey ©NERC. All rights Reserved. The locations of Lilstock, Kilve, East Quantoxhead, Watchet and Blue Anchor Bay are shown.

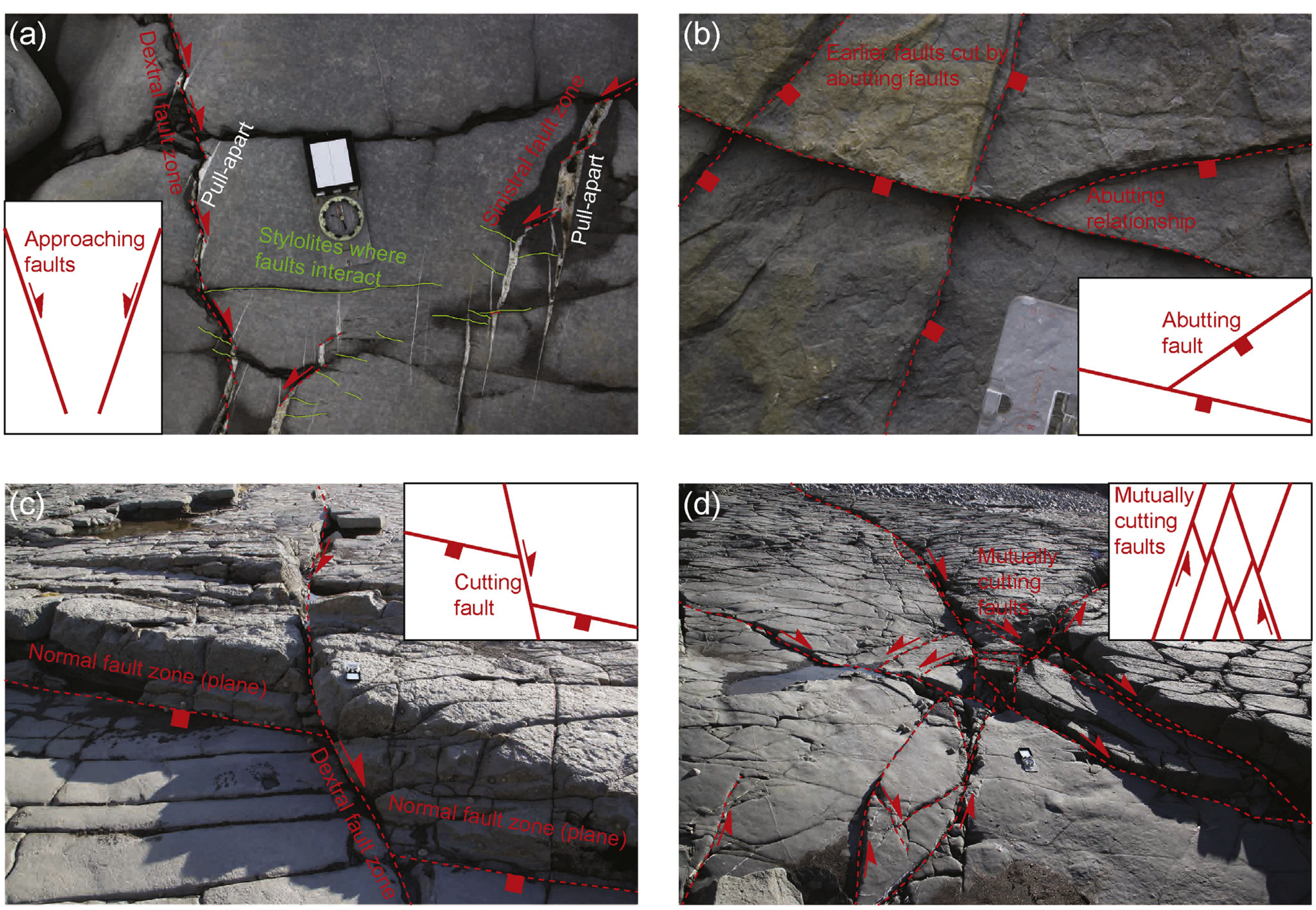

Fig. 5. Examples of faults from the Liassic limestones and shales of Somerset, UK, showing different geometric relationships between the faults. (a) Conjugate strike-slip faults at Kilve that approach each other and interact but do not actually meet. Interaction is indicated by stylolites (green) in the acute bisector between the faults and between segments along the sinistral fault. (b) A normal fault abuts another normal fault on a bedding plane of Liassic limestone at Watchet. Note that this rock was not *in situ*. (c) Oblique view of a strike-slip fault cutting and displacing a normal fault zone at East Quantoxhead. (d) Oblique view of two conjugate strike-slip fault zones at East Quantoxhead that appear to mutually crosscut each other. This is indicated by the intricate pattern of fault segments and areas of relative uplift and subsidence in the interaction zone.(For interpretation of the references to colour in this figure legend, the reader is referred to the web version of this article.)

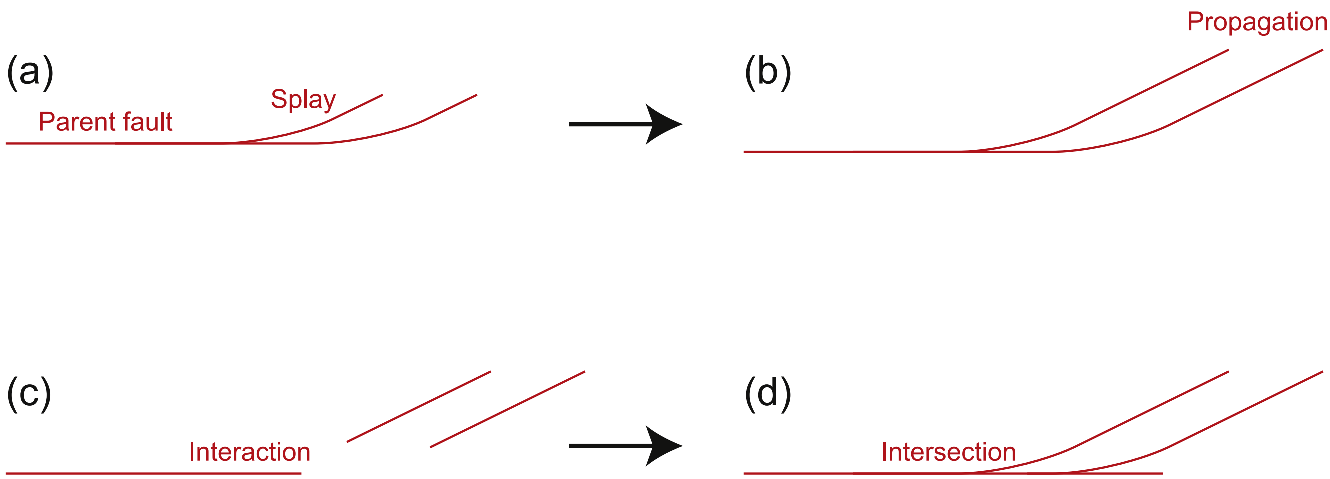

Fig. 6. Schematic figure to represent the development of splaying and approaching faults. (a) and (b) Splaying faults. (a) Splay faults develop at or near the tip of a parent fault. (b) The splay faults continue to propagate away from the parent fault. (c) and (d) Approaching and intersecting faults. (c) Faults approach each other. (d) The faults intersect. The result can appear similar to the splaying faults shown in Fig. 6(b).

50 m of net normal displacement but that has been partially reactivated as a reverse fault (e.g., Whittaker and Green, 1983). Antithetic thrusts occur in the hanging-wall to accommodate steepening of the beds and indicating kinematic interaction with the reverse-reactivated normal fault.

The descriptive schemes illustrated in Figs. 5–12 will start to break down for faults that involve more than one deformation event, especially if there has been a change in displacement direction. For example, an intersection line may be parallel to displacement during normal faulting (Fig. 9a) but will be

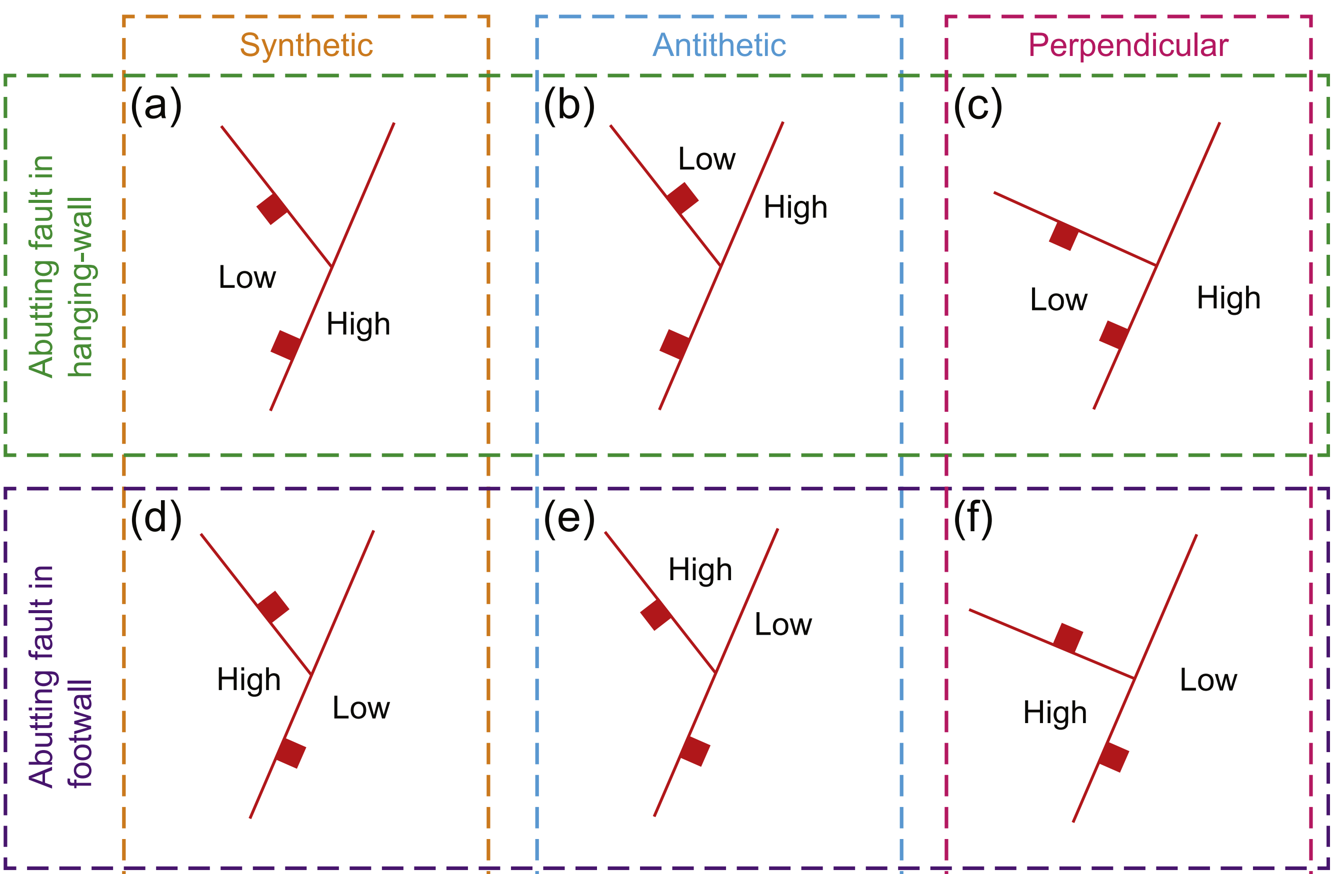

Fig. 7. Characterisation of normal fault interactions based on whether the abutting fault is synthetic or antithetic to the other fault and whether it is in the hanging-wall or footwall of the other fault. (a)–(c) Abutting faults in the hanging-wall. (a) The abutting fault is synthetic to and in the hanging-wall of the fault it abuts. (b) The abutting fault is antithetic to and in the hanging-wall of the fault it abuts. (c) The abutting fault is in the hanging-wall of the fault it abuts, and they are perpendicular to each other. (d)–(f) Abutting faults in the footwall. (d) The abutting fault is synthetic to and in the footwall of the fault it abuts. (e) The abutting fault is antithetic to and in the footwall of the fault it abuts. (f) The abutting fault is in the footwall of the fault it abuts, and they are perpendicular to each other.

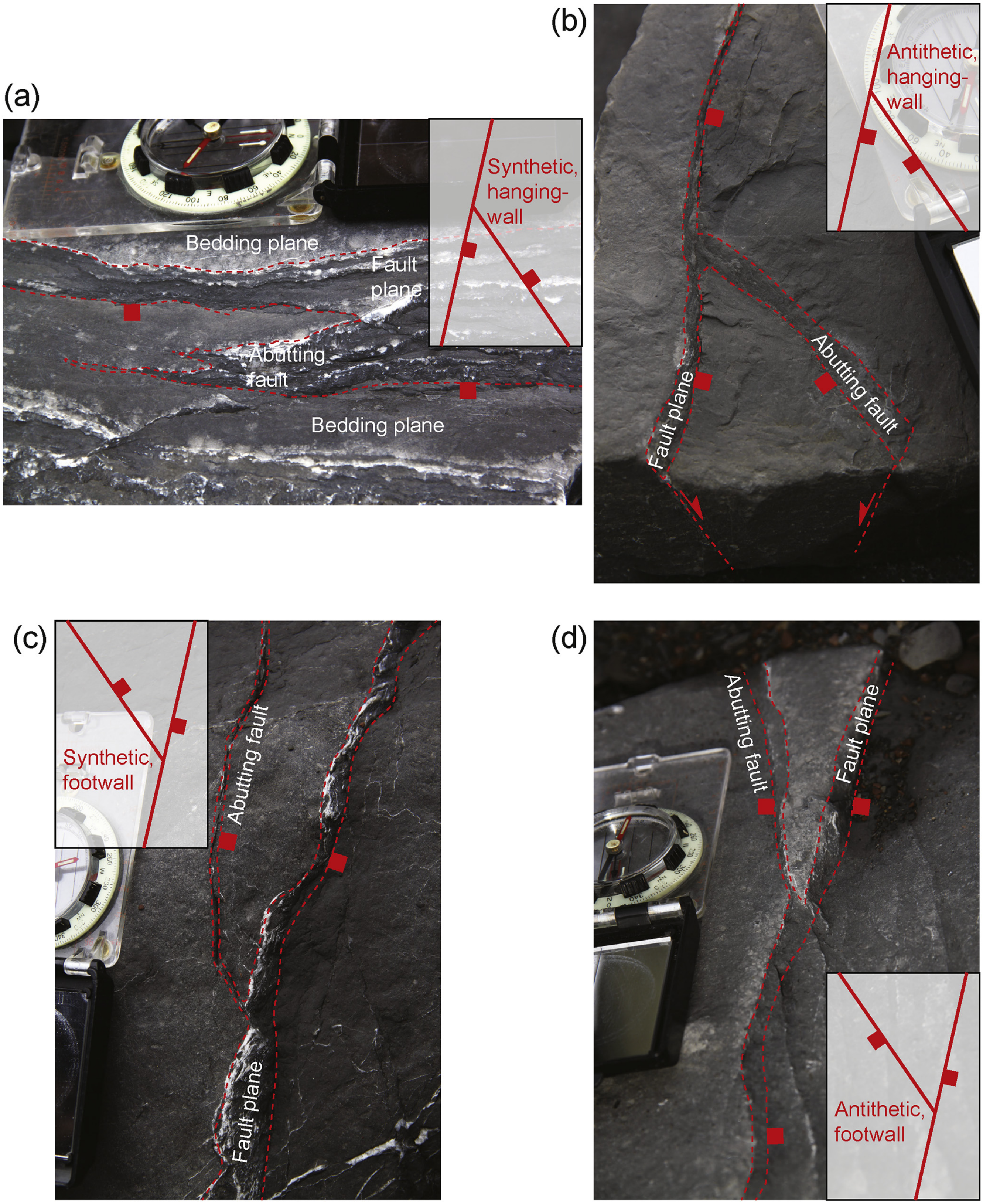

Fig. 8. Examples of normal fault intersections to illustrate some of the geometries shown in Fig. 7, from Watchet, Somerset. Note that these examples were from blocks that were not *in situ*. (a) The abutting fault is synthetic to and in the hanging-wall of the fault it abuts. (b) The abutting fault is antithetic to and in the hanging-wall of the fault it abuts. (c) The abutting fault is synthetic to and in the footwall of the fault it abuts. (d) The abutting fault is antithetic to and in the footwall of the fault it abuts.

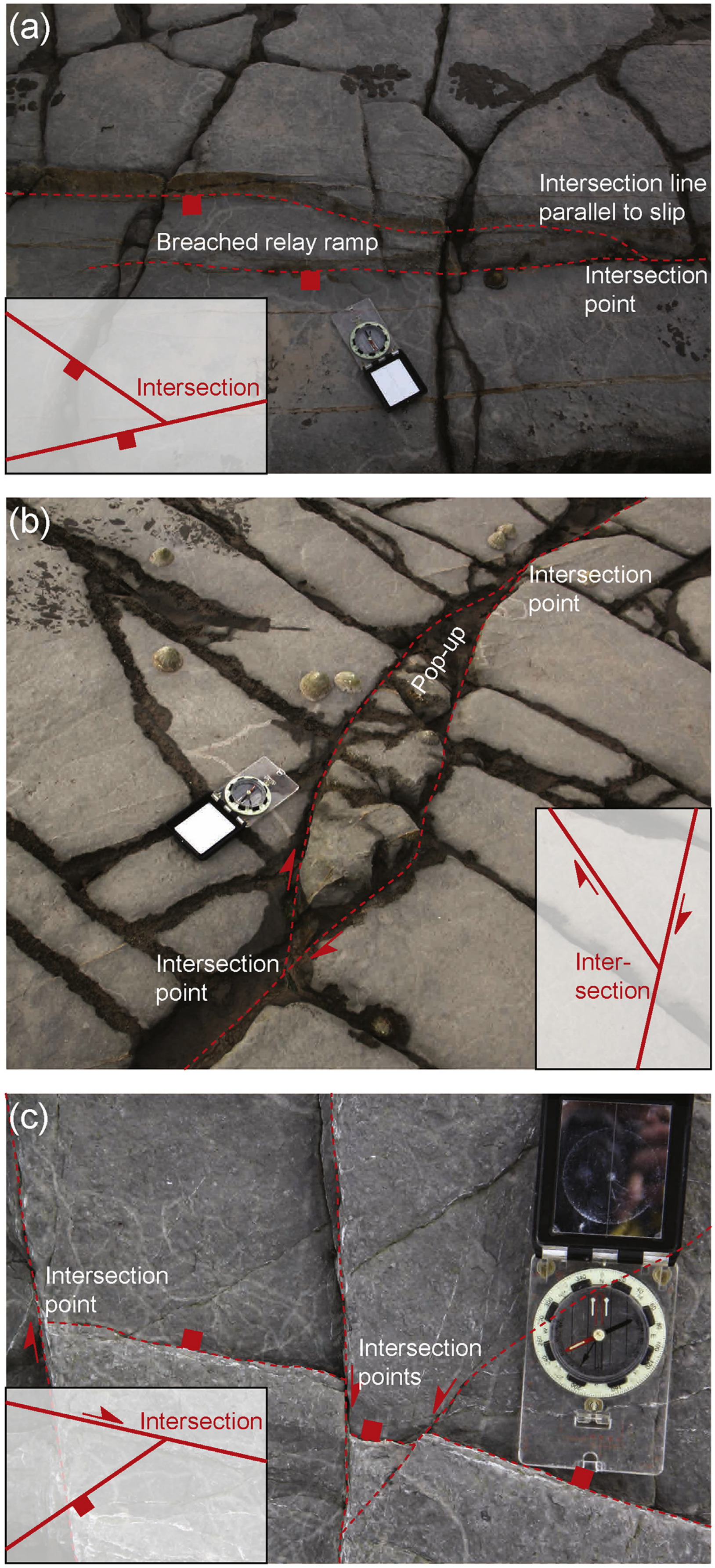

Fig. 9. Examples of faults showing different relationships between their intersection lines and displacement directions, from the Liassic limestones and shales of Somerset, UK. (a) Two stepping normal faults at East Quantoxhead that are linked across a relay ramp by a breaching fault, with the breaching fault connecting with the two stepping faults along intersection lines that are sub-parallel to the fault displacement directions. (b) A contractional bend along a dextral fault zone at East Quantoxhead that has created a pop-up within the lens between the two segments of the fault zone. The intersection lines are approximately perpendicular to the displacement directions of the faults. (c) Faults on a bedding plane in Liassic rocks at Watchet. Note that this rock was not *in situ*. Normal faults are displaced by strike-slip faults. The intersection lines between these faults are sub-parallel to the displacements on the normal faults but approximately perpendicular to the displacements on the strike-slip faults.

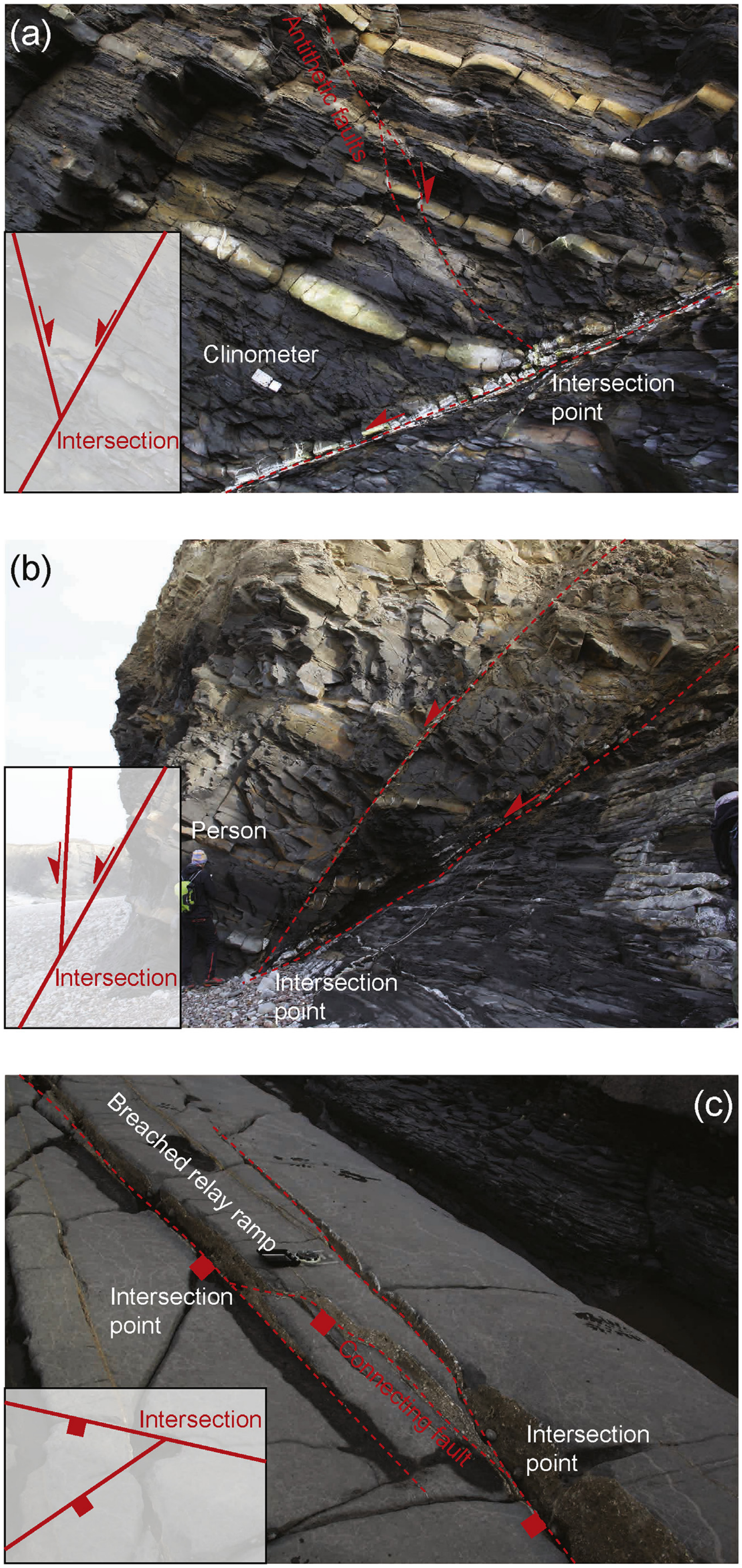

Fig. 10. Examples of normal faults showing different relative shear senses between the faults, from the Liassic limestones and shales at Kilve, Somerset, UK. (a) Antithetic normal faults, where the faults have opposite senses of displacement, approximately perpendicular to the intersection line. (b) Synthetic normal faults, where the faults have the same senses of displacement, approximately perpendicular to the intersection line. (c) Oblique view of intersecting normal faults displacing a limestone bed. They show a “neutral” relationship, where the faults have the same senses of displacement, approximately parallel to the intersection line.

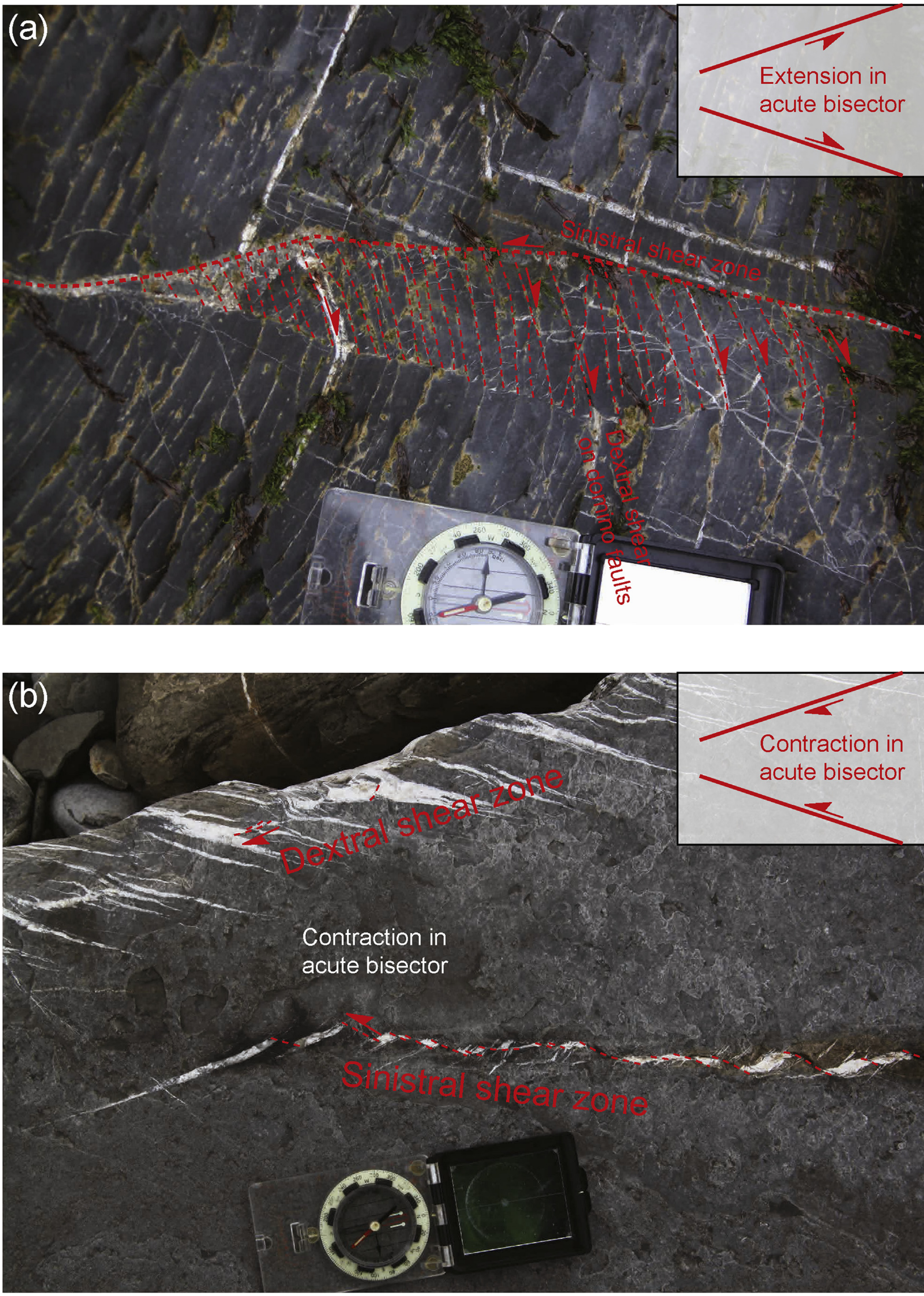

Fig. 11. Examples of faults showing different dominant strains in the acute bisectors of the faults, from the Liassic limestones and shales of Somerset, UK. (a) A joint drag (e.g., Dewey, 1965; Verbeek, 1978) at East Quantoxhead caused by deformation along a sinistral fault in steeply dipping shales. Rotation of the shale laminae is accommodated by small dextral faults, with extension dominating in the acute bisectors between the sinistral fault and the smaller dextral faults, with spaces filled by calcite cement. (b) Conjugate strike-slip faults exposed on a limestone bedding plane Lilstock. There is a tendency for contraction in the acute bisector, although some extension occurs, shown by precipitation of calcite along the fault planes.

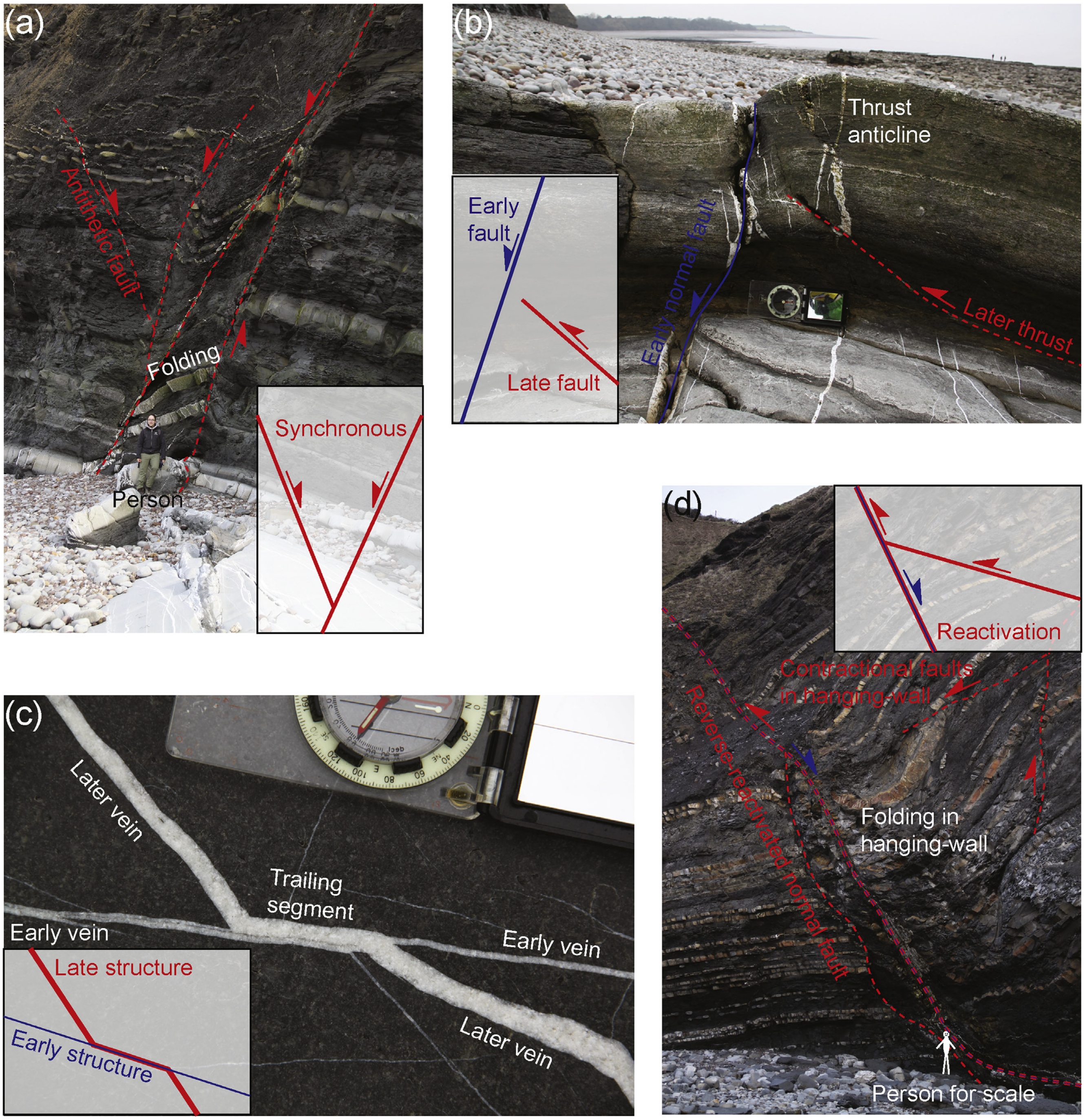

Fig. 12. Examples of faults and veins showing interacting faults with different relative ages, from the Liassic limestones and shales of Somerset, UK. (a) Two intersecting normal faults at Kilve that appear to have been synchronously active, as indicated by the folding of bedding between the faults. (b) A normal and a later thrust fault at Lilstock showing an approaching relationship. (c) Calcite veins on a bedding plane of Liassic limestone at Lilstock. Two later veins intersect and utilise an earlier, with the trailing geometry causing an increase in aperture of the earlier vein between the later veins. (d) The East Quantoxhead fault, which has ~50 m of net normal displacement but that has been partially reactivated as a reverse fault (Whittaker and Green, 1983). Antithetic thrusts occur in the hanging-wall, kinematically interacting with the reverse-reactivated normal fault.

perpendicular to displacement if the faults are reactivated in strike-slip (Fig. 9b). We also acknowledge that other types of relationships between interacting faults may be defined. For example, an early fault may be passively folded by a later fault, which is common behaviour in footwall-propagating thrust systems (e.g., Fig. 13).

7. Displacements along interacting faults

The relationships between interacting and intersecting faults are illustrated by their displacement patterns. A range of different displacement relationships can occur.

7.1. Displacements on synchronously active faults

A fault can influence the displacement pattern of another synchronously active fault with which it interacts (e.g., Muraoka and Kamata, 1983). For example, displacement is transferred between sub-parallel interacting normal faults that step in map view across

Fig. 13. Passive folding of older thrusts in the hanging-walls of lower, later thrusts. St. Brides Bay, Pembrokeshire, Wales.

relay ramps (e.g., Larsen, 1988; Peacock and Sanderson, 1991; Walsh and Watterson, 1991; Huggins et al., 1995; Soliva and Benedicto, 2004). Relay ramps are characterised by high displacement gradients near the tips of the interacting faults, with displacement transferred between the interacting faults. For example, a small fault splaying off a larger fault can have maximum displacement at the intersection line, decreasing towards the tip, whilst the larger fault can show a jump in displacement at the intersection line. Nelson (2006) shows examples of this behaviour.

Peacock (1991, figure 8) shows high displacement gradients towards the tips of approaching, synchronously active strike-slip faults in sub-vertical Silurian turbidites, SW Scotland. In this example, the high displacement gradients appear to be taken up by strain in the wall rocks in the form of compaction of shales and veins in the sandstones. Similarly, the example shown in Fig. 14 shows two approaching normal faults in Somerset, with high displacement gradients at fault tips taken up by rotation of the horst in the area in which they interact.

7.2. *Displacements on non-synchronous faults*

A fault can influence the displacement patterns of another fault, even if they are of different ages. Whilst earlier faults can simply be passively displaced by later faults without their displacements being altered, an earlier fault can act as a mechanical barrier to a later fault (e.g., Duffy et al., 2015), which will tend to increase the displacement gradient of the later fault as it approaches the barrier. Also, some faults show “trailing” geometries and kinematics (Nixon et al., 2014a). “Trailing” is where two new faults are connected via an older fault, on which renewed displacement occurs to connect the two later faults (Peacock et al., 2016). Portions of the early fault are thus re-utilised by the younger abutting faults, transferring displacement onto other younger abutting faults. The older fault therefore has renewed displacement between the younger faults (Fig. 12c).

8. Interaction damage zones

Deformation is commonly concentrated in the zones in which faults interact and intersect. Strain is concentrated in these areas to take up displacement variations along the faults and to accommodate space problems created by fault interaction. This concentrated deformation can be in a range of forms, including minor faults (e.g., Fig. 5d), and veins and stylolites (Fig. 5a). Peacock et al. (2016) therefore define “interaction damage zones” as a general term for the area of deformation caused by the interaction between two or more faults. It is a more general term than “linking-damage zone” of Kim et al. (2004) because it specifically includes deformation between faults of any orientations and relative ages that interact but not necessarily touch each other. Interaction damage zones can be divided into “approaching damage zones” and “intersection-damage zones”. An approaching damage zone is an area of deformation related to interaction between two or more faults that do not intersect (e.g., Fig. 5a). An intersection damage zone is the area of deformation around the intersection point of two or more faults (e.g., Fig. 5d). Interaction- and intersection-damage zones can develop between faults of different ages, e.g., if an earlier fault is a mechanical barrier to the propagation of the later fault.

Interacting and intersecting faults have been shown to influence fluid migration (e.g., Rotevatn et al., 2007, 2009b; Manzocchi et al., 2010) and entrapment (e.g., Gartrell et al., 2004; Rotevatn and Fossen, 2011). We suggest that interaction damage zones can control fluid flow around interacting faults, so these must be

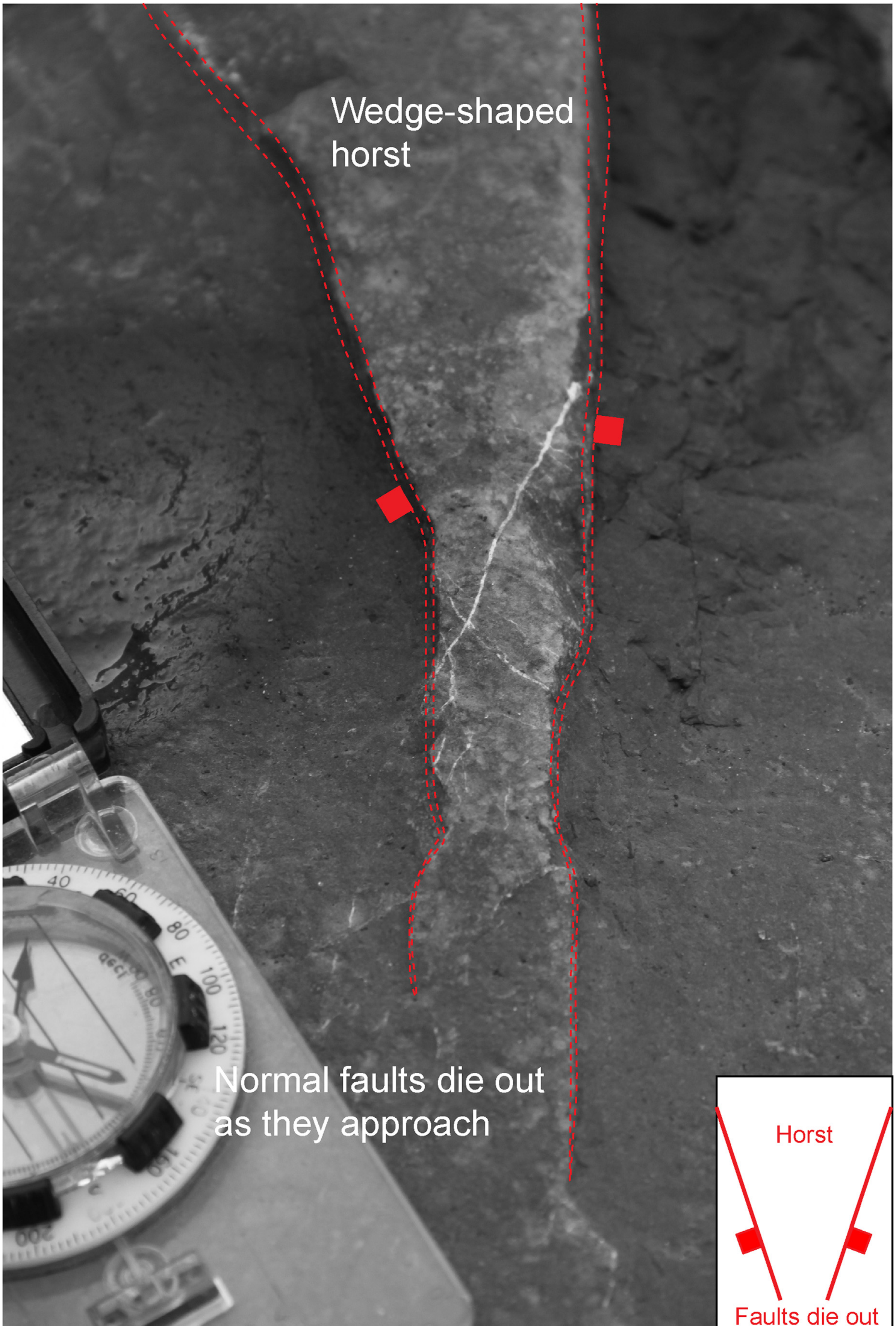

Fig. 14. Two conjugate normal faults, with displacements of the faults dying towards the area in which they interact, from Watchet, Somerset. Note that this block was not *in situ*.

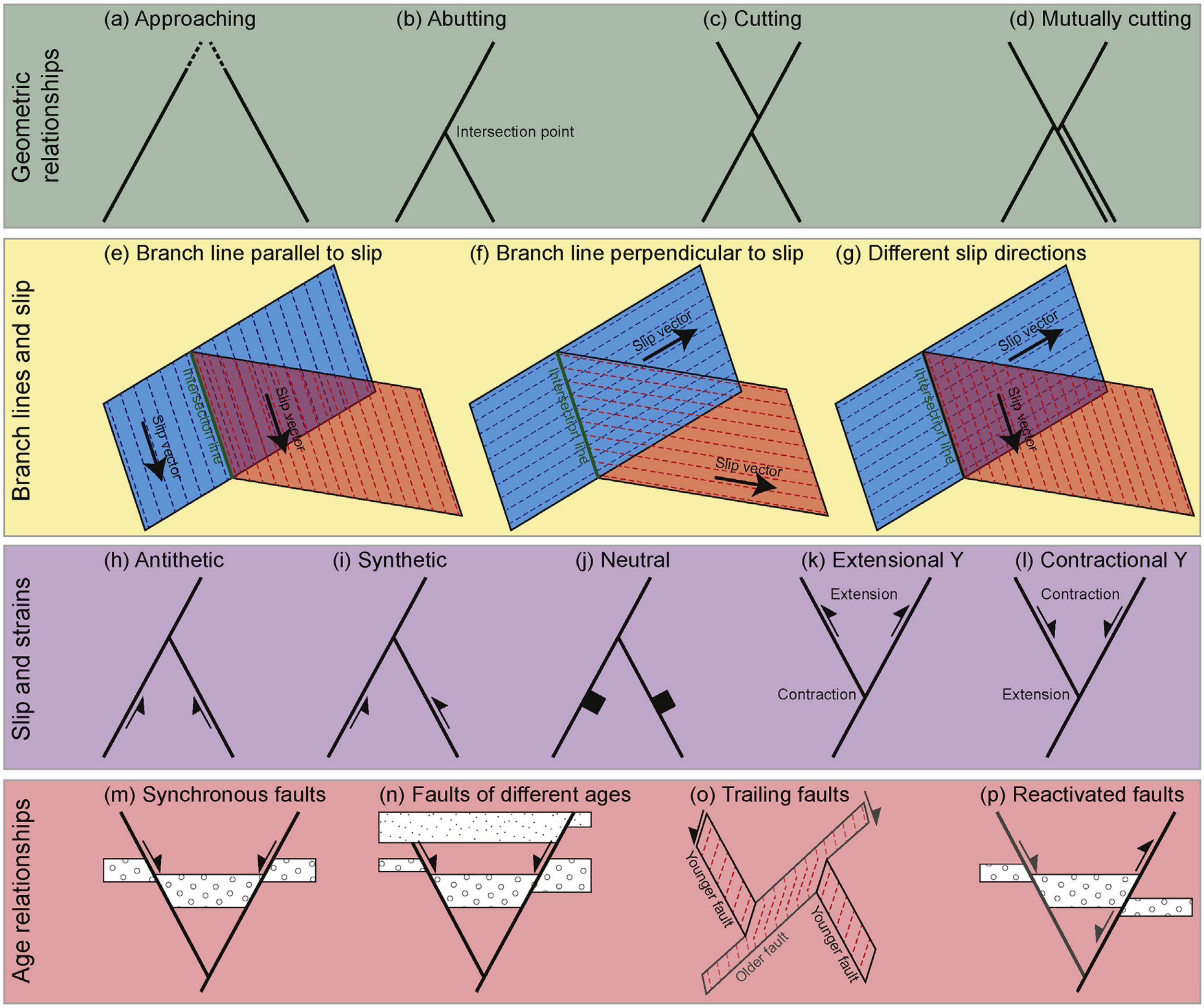

Fig. 15. Classification of intersecting faults. (a) to (d) Classification based on the geometric relationships between the faults. (a) The faults interact as they *approach* each other, but they need not be connected by faults or other fractures (can be similar to the *linkage-damage zone* of Kim et al., 2004). (b) One fault abuts the other. (c) One fault (earlier) is cut by the other (later). (d) The faults mutually crosscut each other. (e) to (g) Classification based on the relationship between the intersection line and the displacement direction. (e) The intersection line is parallel to the displacement direction. (f) The intersection line is perpendicular to the displacement direction. (g) The intersection line is parallel to the displacement direction of one fault and perpendicular to the displacement direction of the other fault. (h) to (l) Classification based on the relative shear senses of the faults and the dominant strains at the interactions. (h) Antithetic relationship, where the faults have opposite senses of displacement. (i) Synthetic relationship, where the faults have the same senses of displacement, approximately perpendicular to the intersection line. (j) Neutral relationship, where the faults have the same senses of displacement, approximately parallel to the intersection line. (k) and (l) Sub-classification for antithetic interactions based on the dominant strain in the acute bisectors of the faults. (k) Extension dominates in the acute bisector, although contraction may dominate in the obtuse bisector. (l) Contraction dominates in the acute bisector, although extension may dominate in the obtuse bisector. (m) to (o) Classification based on the relative ages of the intersecting faults. (m) The faults are synchronous. (n) The faults are different ages. (o) “Trailing” geometry, where part of an earlier fault is reactivated by interaction with later faults. (p) One or both faults have been reactivated.

understood if fluid flow is to be predicted in the subsurface.

9. Effects of fault interaction on subsequent deformation

Faults can act as mechanical barriers that influence subsequent deformation (e.g., Duffy et al., 2015), with *in situ* stresses being perturbed around non-active faults (e.g., Zoback and Richardson, 1996). Such perturbation appears to be particularly acute in fault interaction zones. For example, Bourne and Willemse (2001, figure 7) show perturbed joints within a network of strike-slip faults in Liassic limestones at Nash Point, Vale of Glamorgan, Wales, on the north side of the Bristol Channel Basin, approximately 32 km NW of Kilve, Somerset. This suggests that post-fault deformation and the *in situ* stresses around interacting faults should be considered when predicting both the deformation within interaction damage zones and related fluid migration.

10. Classification scheme

The ways of characterising interacting and intersecting faults described here may be used as the basis for a classification scheme, as summarised in Fig. 15. This classification scheme is based on geometric relationships, angles between the intersection lines and displacement directions, the strain that occurs at and around the interaction or intersection zones, and on the relative age relationships of the interacting faults. This scheme is applicable to any two faults, being independent of such factors as tectonic setting and scale. We suggest that this scheme is a useful tool for analysing fault systems because it emphasises the geometric, kinematic and temporal relationships between the components of a network.

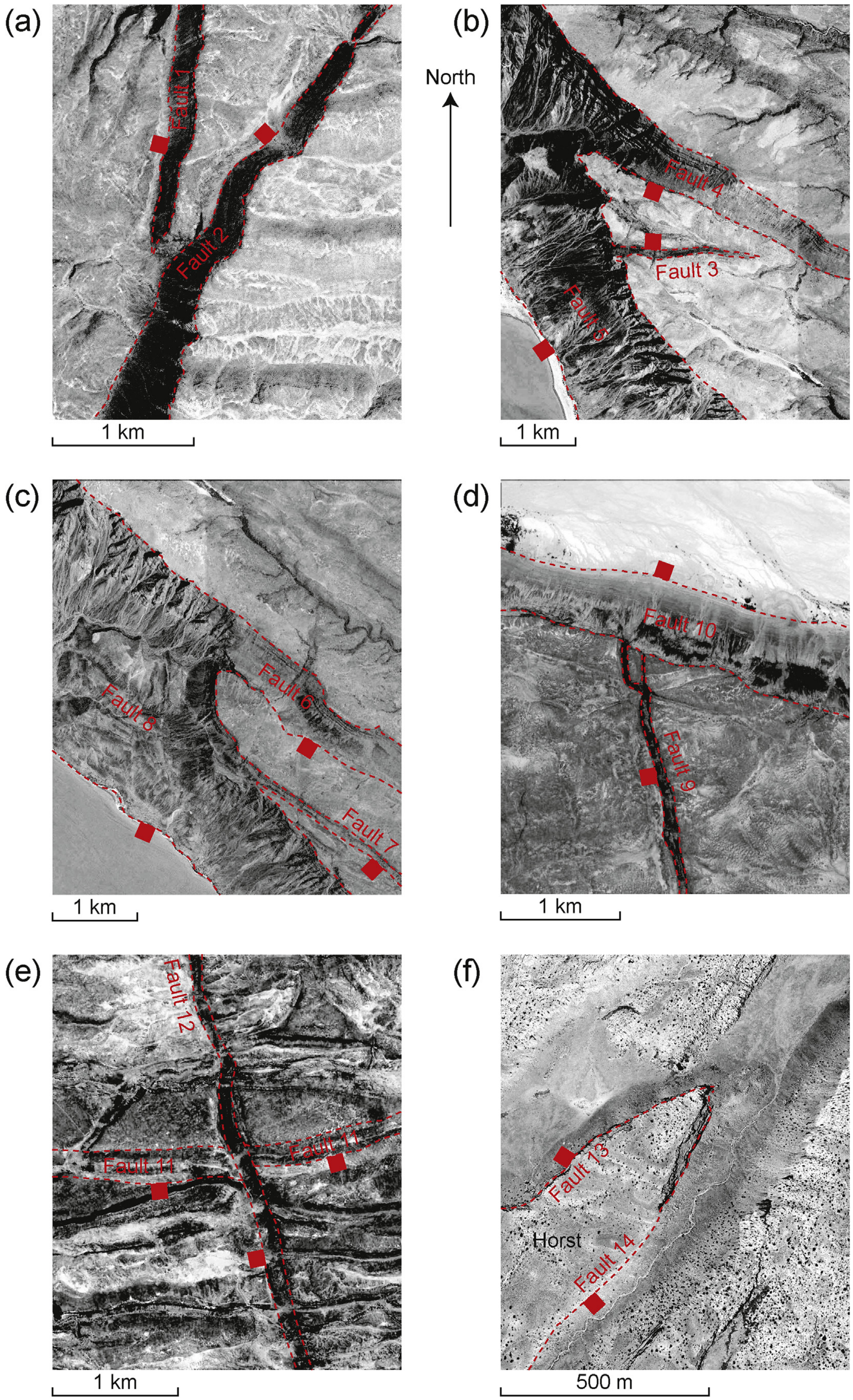

Fig. 16. Examples of normal fault intersections (Fig. 7) from Google Earth. (a) to (e) are from the East African Rift. (a) Synthetic fault 1 in the hanging-wall of fault 2 (11°00′33″, 41°39′46″E). (b) Antithetic fault 3 in the hanging-wall of fault 4. Both are in the footwall of fault 5 (11°35′46″N, 41°40′55″E). (c) Synthetic faults 6 and 7 are in the footwall of fault 8 (11°33′41″N, 41°42′07″E). (d) Antithetic fault 9 is in the footwall of fault 10 (10°57′17″N, 41°51′45″E). (e) Faults 11 and 12 are perpendicular to each other, with fault 11 apparently displaced by fault 12. Each therefore abuts abutting the other in both the hanging-wall and the footwall (10°48′57″N, 41°53′13″E). (f) Antithetic faults 13 and 14 meeting at their tips (38° 5′33″N, 109°55′50″W), from Canyonlands, Utah, USA. Other faults are not marked.

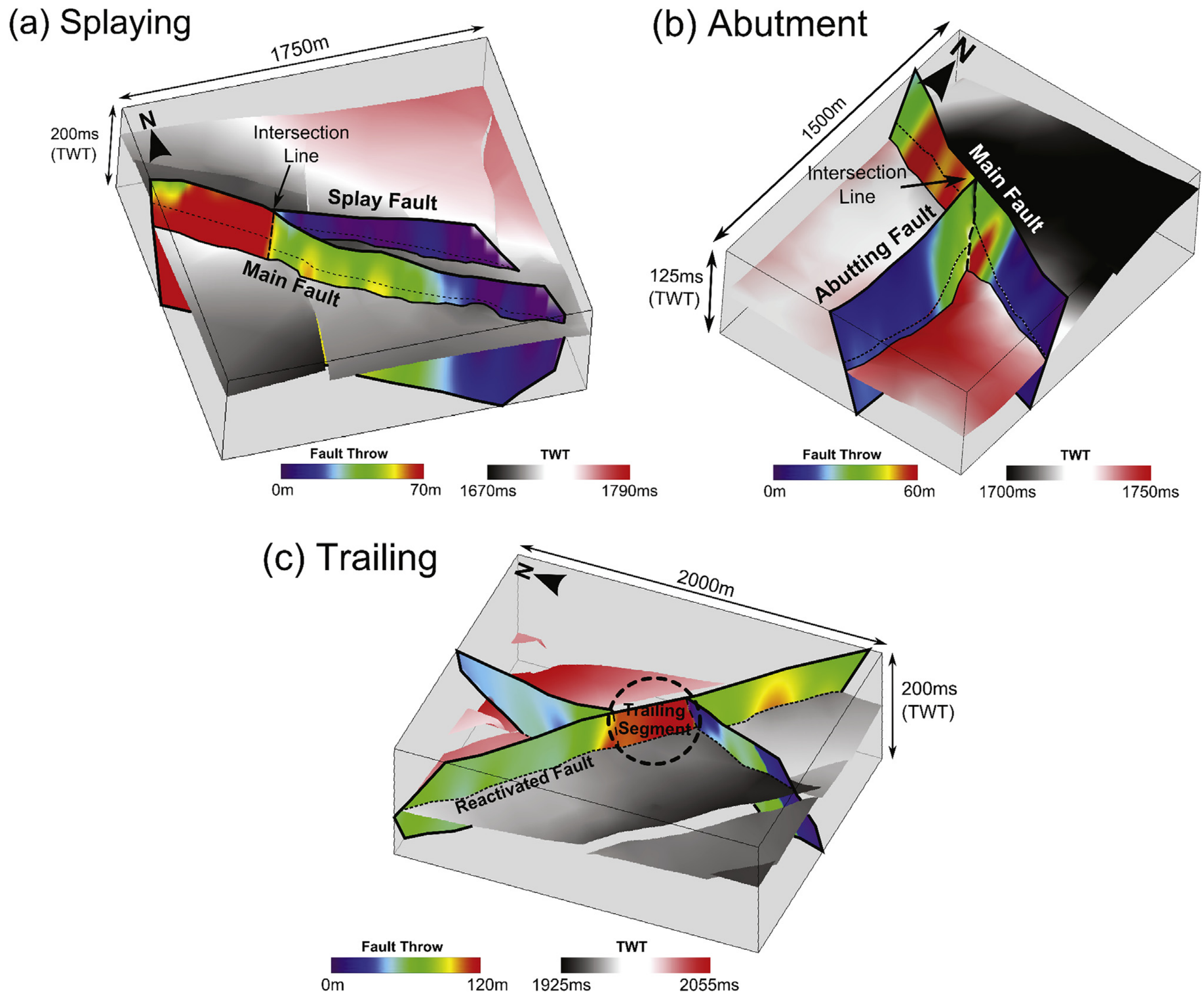

Fig. 17. Examples of interacting faults in a seismic reflection volume from Milne Point, Alaska, modified from Nixon et al. (2014a). The diagrams illustrate the 3-dimensional geometric and kinematic interaction of normal fault planes including. a) A splay fault and its associated main fault. b) A younger fault abuts and locally reactivates an older fault. c) Kinematically linked abutting faults that have locally reactivated an older fault to form a trailing segment. The distribution of throw is contoured onto each fault plane, and illustrates variations around the intersection lines.

11. Scaling of fault interactions

The geometries shown in Figs. 5–12 also occur on much larger faults (Table 1). Self-similarity of fault geometries was first illustrated by Tchalenko (1970), and subsequent work has shown that they exhibit fractal behaviour (e.g., Mandlebrot, 1982; Turcotte, 1989; Gillespie et al., 1993) and show scale invariant geometries at all scales (e.g., Turcotte, 1989; Main, 1996). This suggests that well-exposed small-scale intersecting faults observed in the field can be used to gain useful insights into deformation patterns around along and around much larger intersecting faults. Fig. 16 shows faults examples of interacting normal faults from the East African Rift that illustrate the range of geometries shown in Figs. 7 and 8.

12. The three-dimensional character of fault interaction

The examples from the Mesozoic sedimentary rocks of Somerset, UK, are exposed on rock surfaces, so are approximately two-dimensional. For example, the faults intersect at *intersection points*. In three-dimensions, these intersection points are *intersection lines* (e.g., Peacock et al., 2016). The three-dimensional character of fault intersections is illustrated in Fig. 17. Whilst faults are commonly studied in two-dimensions, especially in the field, it must be remembered that the interactions between faults is a three-dimensional issue. For example, stepping fault segments may be linked out of the plane of observation (e.g., Harding and Lowell, 1979).

13. Conclusions

Various criteria can be used to characterise and classify fault interactions:

- **Geometric relationships**, i.e., where the faults approach but do not intersect, where one fault abuts the other, where the faults mutually crosscut, and where one fault displaces the other. Further characterisation is possible, such as whether interacting dip-slip faults occur in the footwall or hanging-wall of the faults with which they interact, and whether they are synthetic or antithetic.

- The **relationship between the intersection line and the displacement direction**, i.e., whether the intersection line is parallel, perpendicular or oblique to the displacement directions of both faults, or whether the faults have different displacement directions.
- **Displacement and strain in the interaction zone**, i.e., whether the faults are antithetic, synthetic or show a neutral relationship. Characterisation is also possible by the strain that dominates where the faults intersect, i.e., whether extension or contraction dominates in the acute bisector between the faults.
- **Relative age relationships**, i.e., whether the faults are the same age, different ages or if one or both faults have been reactivated.

This scheme can be used as a basis for understanding the stresses and strains that occur around fault interaction, and may therefore help understand the damage that occurs. We define “interaction damage zones” as developing between two or more faults of any relative orientation or age that interact with each other.

Acknowledgements

We are very grateful to Fabrizio Agosta, Ian Alsop and Jonny Imber for their reviews. Kristin Hool and Torill Jordal at NAV are thanked for facilitating DCPP working on a placement at UiB. Nixon is supported by a VISTA scholarship from the Norwegian Academy of Science and Letters. We acknowledge financial support for the ANIGMA project from the Research Council of Norway (project no. 244129/E20) through the ENERGIX program, and from Statoil ASA through the Akademia agreement.

References

Aydin, A., 2000. Fractures, faults, and hydrocarbon entrapment, migration and flow. Mar. Pet. Geol. 17, 797–814.
Aydin, A., Schultz, R.A., 1990. Effect of mechanical interaction on the development of strike-slip faults with echelon patterns. J. Struct. Geol. 12, 123–129.
Bailey, W.R., Walsh, J.J., Manzocchi, T., 2005. Fault populations, strain distribution and basement fault reactivation in the East Pennines Coalfield, UK. J. Struct. Geol. 27, 913–928.
Bastesen, E., Rotevatn, A., 2012. Evolution and structural style of relay zones in layered limestone–shale sequences: insights from the Hammam Faraun Fault Block, Suez rift, Egypt. J. Geol. Soc. Lond. 169, 477–488.
Biddle, K.T., Christie-Blick, N., 1985. Glossary – strike-slip deformation, basin formation, and sedimentation. In: Biddle, K.T., Christie-Blick, N. (Eds.), Strike-slip Deformation, Basin Formation, and Sedimentation, Vol. 37. Society of Economic Mineralogists Special Publication, pp. 375–386.
Bourne, S.J., Willemse, E.J.M., 2001. Elastic stress control on the pattern of tensile fracturing around a small fault network at Nash Point. J. Struct. Geol. 23, 1753–1770.
Bull, J.M., Barnes, P.M., Lamarche, G., Sanderson, D.J., Cowie, P.A., Taylor, S.K., Dix, J.K., 2006. High-resolution record of displacement accumulation on an active normal fault: implications for models of slip accumulation during repeated earthquakes. J. Struct. Geol. 28, 1146–1166.
Butler, R.W.H., 1982. The terminology of structures in thrust belts. J. Struct. Geol. 4, 239–245.
Carne, R.C., Little, T.A., 2012. Geometry and scale of fault segmentation and deformational bulging along an active oblique-slip fault (Wairarapa fault, New Zealand). Bull. Geol. Soc. Am. 124, 1365–1381.
Cartwright, J.A., Trudgill, B.D., Mansfield, C.S., 1995. Fault growth by segment linkage: an explanation for scatter in maximum displacement and trace length data from the Canyonlands Grabens of SE Utah. J. Struct. Geol. 17, 1319–1326.
Choi, J.H., Edwards, P., Ko, K., Kim, Y.S., 2016. Definition and classification of fault damage zones: a review and a new methodological approach. Earth-Sci. Rev. 152, 70–87.
Chorowicz, J., 2005. The East African rift system. J. Afr. Earth Sci. 43, 379–410.
Crider, J.G., Peacock, D.C.P., 2004. Initiation of brittle faults in the upper crust: a review of field observations. J. Struct. Geol. 26, 691–707.
Curewitz, D., Karson, J.A., 1997. Structural settings of hydrothermal outflow: fracture permeability maintained by fault propagation and interaction. J. Volcanol. Geotherm. Res. 79, 149–168.
Dart, C.J., McClay, K., Hollings, P.N., 1995. 3D analysis of inverted extensional fault systems, southern Bristol Channel basin, UK. In: Buchanan, J.G., Buchanan, P.G. (Eds.), Basin inversion, Special Publications, Vol. 88. Geological Society, London, pp. 393–413.
Dewey, J.F., 1965. Nature and origin of kink bands. Tectonophysics 1, 459–494.
Ding, X., Liu, G., Sun, M., Wang, P., 2013. Origin of polygonal fault systems: a case from the Sanzhao sag in the Songliao Basin, East China. Pet. Explor. Dev. 40, 333–343.
Duffy, O.B., Bell, R.E., Jackson, C.A.L., Gawthorpe, R.L., Whipp, P.S., 2015. Fault growth and interactions in a multiphase rift fault network: the Horda Platform, Norwegian North Sea. J. Struct. Geol. 80, 99–119.
Ehteshami-Moinabadi, M., 2014. Fault zone migration by footwall shortcut and recumbent folding along an inverted fault: example from the Mosha Fault, Central Alborz, Northern Iran. Can. J. Earth Sci. 51, 825–836.
Ferrill, D.A., Morris, A.P., McGinnis, R.N., 2009. Crossing conjugate normal faults in field exposures and seismic data. Am. Assoc. Pet. Geol. Bull. 93, 1471–1488.
Fossen, H., Rotevatn, A., 2016. Fault linkage and relay structures in extensional settings – a review. Earth-Sci. Rev. 154, 14–28.
Fossen, H., Johansen, T.E.S., Hesthammer, J., Rotevatn, A., 2005. Fault interaction in porous sandstone and implications for reservoir management; examples from southern Utah. Am. Assoc. Pet. Geol. Bull. 89, 1593–1606.
Frankowicz, E., McClay, K.R., 2010. Extensional fault segmentation and linkages, Bonaparte basin, outer North West Shelf, Australia. Am. Assoc. Pet. Geol. Bull. 94, 977–1010.
Gartrell, A., Zhang, Y., Lisk, M., Dewhurst, D., 2004. Fault intersections as critical hydrocarbon leakage zones: integrated field study and numerical modelling of an example from the Timor Sea. Aust. Mar. Pet. Geol. 21, 1165–1179.
Gartrell, A., Bailey, W.R., Brincat, M., 2006. A new model for assessing trap integrity and oil preservation risks associated with postrift fault reactivation in the Timor Sea. Am. Assoc. Pet. Geol. Bull. 90, 1921–1944.
Gawthorpe, R.L., Jackson, C.A.L., Young, M.J., Sharp, I.R., Moustafa, A.R., Leppard, C.W., 2003. Normal fault growth, displacement localisation and the evolution of normal fault populations: the Hammam Faraun fault block, Suez rift, Egypt. J. Struct. Geol. 25, 883–895.
Giba, M., Walsh, J.J., Nicol, A., 2012. Segmentation and growth of an obliquely reactivated normal fault. J. Struct. Geol. 39, 253–267.
Gillespie, P.A., Howard, C.B., Walsh, J.J., Watterson, J., 1993. Measurement and characterization of spatial distributions of fractures. Tectonophysics 226, 113–141.
Glen, R.A., Hancock, P.L., Whittaker, A., 2005. Basin inversion by distributed deformation: the southern margin of the Bristol Channel Basin, England. J. Struct. Geol. 27, 2113–2134.
Griffiths, P.S., 1980. Box-fault systems and ramps: atypical associations of structures from the eastern shoulder of the Kenya Rift. Geol. Mag. 117, 579–586.
Guest, B., Axen, G.J., Lam, P.S., Hassanzadeh, J., 2006. Late Cenozoic shortening in the west-central Alborz Mountains, northern Iran, by combined conjugate strike-slip and thin-skinned deformation. Geosphere 2, 35–52.
Harding, T.P., Lowell, J.D., 1979. Structural styles, their plate-tectonic habitats, and hydrocarbon traps in petroleum provinces. Bull. Am. Assoc. Pet. Geol. 63, 1016–1058.
Hesthammer, J., Landro, M., Fossen, H., 2001. Use and abuse of seismic data in reservoir characterisation. Mar. Pet. Geol. 18, 635–655.
Hibsch, C., Jarrige, J.J., Cushing, E.M., Mercier, J., 1995. Palaeostress analysis, a contribution to the understanding of basin tectonics and geodynamic evolution. Example of the Permian/Cenozoic tectonics of Great Britain and geodynamic implications in western Europe. Tectonophysics 252, 103–136.
Horsfield, W.T., 1980. Contemporaneous movement along crossing conjugate normal faults. J. Struct. Geol. 2, 305–310.
Huggins, P., Watterson, J., Walsh, J.J., Childs, C., 1995. Relay zone geometry and displacement transfer between normal faults recorded in coal-mine plans. J. Struct. Geol. 17, 1741–1755.
Jolley, S.J., Fisher, Q.J., Ainsworth, R.B., 2010. Reservoir compartmentalization: an introduction. In: Jolley, S.J., Fisher, Q.J., Ainsworth, R.B., Vrolijk, P.J., Delisle, S. (Eds.), Reservoir Compartmentalization, Special Publications, Vol. 347. Geological Society, London, pp. 1–8.
Kattenhorn, S.A., Aydin, A., Pollard, D.D., 2000. Joints at high angles to normal fault strike: an explanation using 3-D numerical models of fault-perturbed stress fields. J. Struct. Geol. 22, 1–23.
Katz, Y., Weinberger, R., Aydin, A., 2004. Geometry and kinematic evolution of Riedel shear structures, Capitol Reef National Park, Utah. J. Struct. Geol. 26, 491–501.
Kelly, P.G., Sanderson, D.J., Peacock, D.C.P., 1998. Linkage and evolution of conjugate strike-slip fault zones in limestones of Somerset and Northumbria. J. Struct. Geol. 20, 1477–1493.
Kelly, P.G., McGurk, A., Peacock, D.C.P., Sanderson, D.J., 1999. Reactivated normal faults in the Mesozoic of the Somerset coast, and the role of fault scale in reactivation. J. Struct. Geol. 21, 493–509.
Kim, Y.S., Peacock, D.C.P., Sanderson, D.J., 2003. Strike-slip faults and damage zones at Marsalforn, Gozo Island, Malta. J. Struct. Geol. 25, 793–812.
Kim, Y.S., Peacock, D.C.P., Sanderson, D.J., 2004. Fault damage zones. J. Struct. Geol. 26, 503–517.
Knipe, R.J., 1992. Faulting processes and fault seal. In: Larsen, R.M., Brekke, H., Larsen, B.T., Tallerass, E. (Eds.), Structural and Tectonic Modelling and its Application to Petroleum Geology, vol. 1. Norwegian Petroleum Society Special Publications, pp. 325–342.
Larsen, P.-H., 1988. Relay structures in a Lower Permian basement-involved

extension system, East Greenland. J. Struct. Geol. 10, 3–8.
Leeder, M.R., Jackson, J.A., 1993. The interaction between normal faulting and drainage in active extensional basins, with examples from the western United States and central Greece. Basin Res. 5, 79–102.
Lonergan, L., Cartwright, J., Jolly, R., 1998. The geometry of polygonal fault systems in Tertiary mudrocks of the North Sea. J. Struct. Geol. 20, 529–548.
Maerten, L., 2000. Variation in slip on intersecting normal faults: implications for paleostress inversion. J. Geophys. Res. 105, 25565–25565.
Maerten, L., Pollard, D.D., Maerten, F., 2001. Digital mapping of three-dimensional structures of the Chimney Rock fault system, central Utah. J. Struct. Geol. 23, 585–592.
Maerten, L., Gillespie, P., Pollard, D.D., 2002. Effects of local stress perturbation on secondary fault development. J. Struct. Geol. 24, 145–153.
Main, I., 1996. Statistical physics, seismogenesis, and seismic hazard. Rev. Geophys. 34, 433–462.
Mandlebrot, B.B., 1982. The Fractal Geometry of Nature. W.H. Freeman, San Francisco.
Manzocchi, T., Walsh, J.J., Nell, P., Yielding, G., 1999. Fault transmissibility multipliers for flow simulation models. Pet. Geosci. 5, 53–63.
Manzocchi, T., Childs, C., Walsh, J.J., 2010. Faults and fault properties in hydrocarbon flow models. Geofluids 10, 94–113.
Michie, E.A.H., Haines, T.J., Healy, D., Neilson, J.E., Timms, N.E., Wibberley, C.A.J., 2014. Influence of carbonate facies on fault zone architecture. J. Struct. Geol. 65, 82–99.
Mollema, P.N., Antonellini, M., 1999. Development of strike-slip faults in the dolomites of the Sella Group, northern Italy. J. Struct. Geol. 21, 273–292.
Molnar, P., Tapponnier, P., 1975. Cenozoic tectonics of Asia: effects of a continental collision. Science 189, 419–426.
Moore, G.F., Boston, B.B., Sacks, A.F., Saffer, D.M., 2013. Analysis of normal fault populations in the Kumano Forearc Basin, Nankai Trough, Japan: 1. Multiple orientations and generations of faults from 3-D coherency mapping. Geochem. Geophys. Geosystems 14, 1989–2002.
Morley, C.K., 2014. Outcrop examples of soft-sediment deformation associated with normal fault terminations in deepwater, Eocene turbidites: a previously undescribed conjugate fault termination style? J. Struct. Geol. 69, 189–208.
Morley, C.K., Nelson, R.A., Patton, T.L., Munn, S.G., 1990. Transfer zones in the East African rift system and their relevance to hydrocarbon exploration in rifts. Am. Assoc. Pet. Geol. Bull. 74, 1234–1253.
Muraoka, H., Kamata, H., 1983. Displacement distribution along minor fault traces. J. Struct. Geol. 5, 483–495.
Needham, D.T., Yielding, G., Freeman, B., 1996. Analysis of fault geometry and displacement patterns. In: Buchanan, E.G., Nieuwland, D.A. (Eds.), Modern Developments in Structural Interpretation, Validation and Modelling, Special Publication vol. 99. Geological Society, London, pp. 189–199.
Nelson, M.A., 2006. 3D Geometry and Kinematics of Non-colinear Fault Intersections (Ph.D. thesis). Cardiff University, U.K.
Nemčok, M., Gayer, R., Miliorizos, M., 1995. Structural analysis of the inverted Bristol Channel Basin: implications for the geometry and timing of fracture porosity. In: Buchanan, J.G., Buchanan, P. (Eds.), Basin Inversion, Special Publications, vol. 88. Geological Society, London, pp. 355–392.
Nicol, A., Walsh, J.J., Watterson, J., Bretan, P.G., 1995. Three-dimensional geometry and growth of conjugate normal faults. J. Struct. Geol. 17, 847–862.
Nicol, A., Childs, C., Walsh, J.J., Schafer, K.W., 2013. A geometric model for the formation of deformation band clusters. J. Struct. Geol. 55, 21–33.
Nixon, C.W., Sanderson, D.J., Bull, J.M., 2011. Deformation within a strike-slip fault network at Westward Ho!, Devon U.K.: domino vs conjugate faulting. J. Struct. Geol. 33, 833–843.
Nixon, C.W., Sanderson, D.J., Dee, S., Bull, J.M., Humphreys, R., Swanson, M., 2014a. Fault interactions and reactivation within a normal fault network at Milne Point, Alaska. Am. Assoc. Pet. Geol. Bull. 98, 2081–2107.
Nixon, C.W., Bull, J.M., Sanderson, D.J., 2014b. Localized vs distributed deformation associated with the linkage history of an active normal fault, Whakatane Graben, New Zealand. J. Struct. Geol. 69, 266–280.
Nur, A., Ron, H., Scott, O., 1989. Mechanics of distributed fault and block rotation. In: Kissel, C., Laj, C. (Eds.), Paleomagnetic Rotations and Continental Deformation, NATO ASI Series C, vol. 254, pp. 209–228.
Odonne, F., Massonnat, G., 1992. Volume loss and deformation around conjugate fractures: comparison between a natural example and analog experiments. J. Struct. Geol. 14, 963–972.
Paton, D.A., Underhill, J.R., 2004. Role of crustal anisotropy in modifying the structural and sedimentological evolution of extensional basins: the Gamtoos Basin, South Africa. Basin Res. 16, 339–359.
Peacock, D.C.P., 1991. Displacements and segment linkage in strike-slip fault zones. J. Struct. Geol. 13, 1025–1035.
Peacock, D.C.P., 2001. The temporal relationship between joints and faults. J. Struct. Geol. 23, 329–341.
Peacock, D.C.P., 2002. Propagation, interaction and linkage in normal fault systems. Earth-Sci. Rev. 58, 121–142.
Peacock, D.C.P., Sanderson, D.J., 1991. Displacements, segment linkage and relay ramps in normal fault zones. J. Struct. Geol. 13, 721–733.
Peacock, D.C.P., Sanderson, D.J., 1992. Effects of Layering and Anisotropy on Fault Geometry, vol. 149. Journal of the Geological Society, London, pp. 793–802.
Peacock, D.C.P., Sanderson, D.J., 1994. Geometry and development of relay ramps in normal fault systems. Am. Assoc. Pet. Geol. Bull. 78, 147–165.
Peacock, D.C.P., Sanderson, D.J., 1995. Strike-slip relay ramps. J. Struct. Geol. 17, 1351–1360.
Peacock, D.C.P., Sanderson, D.J., 1999. Deformation history and basin-controlling faults in the Mesozoic sedimentary rocks of the Somerset coast. Proc. Geol. Assoc. 110, 41–52.
Peacock, D.C.P., Zhang, X., 1994. Field examples and numerical modelling of oversteps and bends along normal faults in cross-section. Tectonophysics 234, 147–167.
Peacock, D.C.P., Nixon, C.W., Rotevatn, A., Sanderson, D.J., Zuluaga, L.F., 2016. Glossary of fault and fracture networks. J. Struct. Geol. 92, 12–29.
Pizzi, A., Garaldini, F., 2009. Pre-existing cross-structures and active fault segmentation in the north-central Apennines (Italy). Tectonophysics 467, 304–319.
Platt, J.P., Becker, T.W., 2013. Kinematics of rotating panels of E-W faults in the San Andreas system: what can we tell from geodesy? Geophys. J. Int. 194, 1295–1301.
Proffett, J.M., 1977. Cenozoic geology of the Yerington district, Nevada, and implications for the nature and origin of Basin and Range faulting. Bull. Geol. Soc. Am. 88, 247–266.
Putz-Perrier, M.W., Sanderson, D.J., 2010. Distribution of faults and extensional strain in fractured carbonates of the North Malt Graben. Am. Assoc. Pet. Geol. Bull. 94, 435–456.
Rawnsley, K.D., Peacock, D.C.P., Rives, T., Petit, J.-P., 1998. Jointing in the Mesozoic sediments around the Bristol Channel Basin. J. Struct. Geol. 20, 1641–1661.
Rodgers, D.A., 1980. Analysis of pull-apart basin development produced by en echelon strike-slip faults. In: Balance, P.F., Reading, H.G. (Eds.), Sedimentation in Oblique-slip Mobile Zones, Vol. 4. International Association of Sedimentologists Special Publication, pp. 27–41.
Rotevatn, A., Fossen, H., 2011. Simulating the effect of subseismic fault tails and process zones in a siliciclastic reservoir analogue: implications for aquifer support and trap definition. Mar. Pet. Geol. 28, 1648–1662.
Rotevatn, A., Buckley, S.J., Howell, J.A., Fossen, H., 2009a. Overlapping faults and their effect on fluid flow in different reservoir types: a LIDAR-based outcrop modeling and flow simulation study. Am. Assoc. Pet. Geol. Bull. 93, 407–427.
Rotevatn, A., Tveranger, J., Howell, J.A., Fossen, H., 2009b. Dynamic investigation of the effect of a relay ramp on simulated fluid flow: geocellular modelling of the Delicate Arch Ramp, Utah. Pet. Geosci. 15, 45–58.
Rotevatn, A., Fossen, H., Hesthammer, J., Aas, T.E., Howell, J.A., 2007. Are relay ramps conduits for fluid flow? Structural analysis of a relay ramp in Arches National Park, Utah. In: Lonergan, L., Jolly, R.J.H., Sanderson, D.J., Rawnsley, K. (Eds.), Fractured Reservoirs, Special Publications Vol. 270. Geological Society, London, pp. 55–71.
Soliva, R., Benedicto, A., 2004. A linkage criterion for segmented normal faults. J. Struct. Geol. 26, 2251–2267.
Taylor, M., Peltzer, G., 2006. Current slip rates on conjugate strike-slip faults in central Tibet using synthetic aperture radar interferometry. J. Geophys. Res. 111. B12402–B12402.
Tapponnier, P., Molnar, P., 1977. Active faulting and tectonics in China. J. Geophys. Res. 82, 2905–2930.
Tchalenko, J.S., 1970. Similarities between shear zones of different magnitudes. Bull. Geol. Soc. Am. 81, 1625–1640.
ten Veen, J.H., Boulton, S.J., Alçiçek, M.C., 2009. From palaeotectonics to neotectonics in the Neotethys realm: the importance of kinematic decoupling and inherited structural grain in SW Anatolia (Turkey). Tectonophysics 473, 261–281.
Tesfaye, S., Rowan, M.G., Mueller, K., Trudgill, B.D., Harding, D.J., 2008. Relay and accommodation zones in the Dobe and Hanle grabens, central Afar, Ethiopia and Djibouti. J. Geol. Soc. Lond. 165, 535–547.
Tewksbury, B.J., Hogan, J.P., Kattenhorn, S.A., Mehrtens, C.J., Tarabees, E.A., 2014. Polygonal faults in chalk: insights from extensive exposures of the Khoman Formation, Western Desert, Egypt. Geology 42, 479–482.
Turcotte, D.L., 1989. Fractals in geology and geophysics. Pure Appl. Geophys. 131, 171–219.
Underhill, J.R., Patterson, S., 1998. Genesis of tectonic inversion structures: seismic evidence for the development of key structures along the Purbeck-Isle of Wight Disturbance. J. Geol. Soc. Lond. 155, 975–992.
Vandycke, S., 2002. Palaeostress records in Cretaceous formations in NW Europe: extensional and strike-slip events in relations with Cretaceous-Tertiary inversion tectonics. Tectonophysics 357, 119–136.
Vandycke, S., Bergerat, F., 2001. Brittle tectonic structures and palaeostress analysis in the Isle of Wight, Wessex basin, southern England. J. Struct. Geol. 23, 393–406.
Verbeek, E.R., 1978. Kink bands in the Somport slates, west-central Pyrenees, France and Spain. Bull. Geol. Soc. Am. 89, 814–824.
Walsh, J.J., Watterson, J., 1991. Geometric and kinematic coherence and scale effects in normal fault systems. In: Roberts, A.M., Yielding, G., Freeman, B. (Eds.), The Geometry of Normal Faults, Special Publications, Vol. 56. Geological Society, London, pp. 193–203.
Walsh, J.J., Watterson, J., Bailey, W.R., Childs, C., 1999. Fault relays, bends and branch-lines. J. Struct. Geol. 21, 1019–1026.
Whittaker, A., 1972. The Watchet Fault – a post-Liassic transcurrent reverse fault. Bull. Geol. Survey G. B. 41, 75–80.
Whittaker, A., Green, G.W., 1983. Geology of the Country Around Weston-super-mare. Memoir of the Geological Survey of Great Britain, Sheet 279 and parts of 263 and 295.
Wilcox, R.E., Harding, T.P., Seely, D.R., 1973. Basic wrench tectonics. Am. Assoc. Pet.

Geol. Bull. 57, 74–96.
Willemse, E.J.M., Peacock, D.C.P., Aydin, A., 1997. Nucleation and growth of strike-slip faults in limestone. J. Struct. Geol. 19, 1461–1477.
Woodcock, N.H., Fischer, M., 1986. Strike-slip duplexes. J. Struct. Geol. 8, 725–735.
Woodcock, N.H., Rickards, B., 2003. Transpressive duplex and flower structure: dent fault system, NW England. J. Struct. Geol. 25, 1981–1992.
Zoback, M.L., Richardson, R.M., 1996. Stress perturbation associated with the Amazonas and other ancient continental rifts. J. Geophys. Res. 101, 5459–5475.